remote sensing

MDPI

Article

Detection of Grassland Mowing Events for Germany by Combining Sentinel-1 and Sentinel-2 Time Series

Sophie Reinermann [1,*], Ursula Gessner [2], Sarah Asam [2], Tobias Ullmann [3], Anne Schucknecht [4] and Claudia Kuenzer [1,2]

[1] Department of Remote Sensing, Institute of Geography and Geology, University of Würzburg, 97074 Wuerzburg, Germany; claudia.kuenzer@dlr.de
[2] German Remote Sensing Data Center (DFD), Earth Observation Center (EOC), German Aerospace Center (DLR), 82234 Wessling, Germany; ursula.gessner@dlr.de (U.G.); sarah.asam@dlr.de (S.A.)
[3] Department of Physical Geography, Institute of Geography and Geology, University of Würzburg, 97074 Wuerzburg, Germany; tobias.ullmann@uni-wuerzburg.de
[4] Karlsruhe Institute of Technology (KIT), Institute of Meteorology and Climate Research—Atmospheric Environmental Research, 82467 Garmisch-Partenkirchen, Germany; anne.schucknecht@kit.edu
* Correspondence: sophie.reinermann@dlr.de

Abstract: Grasslands cover one-third of the agricultural area in Germany and play an important economic role by providing fodder for livestock. In addition, they fulfill important ecosystem services, such as carbon storage, water purification, and the provision of habitats. These ecosystem services usually depend on the grassland management. In central Europe, grasslands are grazed and/or mown, whereby the management type and intensity vary in space and time. Spatial information on the mowing timing and frequency on larger scales are usually not available but would be required in order to assess the ecosystem services, species composition, and grassland yields. Time series of high-resolution satellite remote sensing data can be used to analyze the temporal and spatial dynamics of grasslands. Within this study, we aim to overcome the drawbacks identified by previous studies, such as optical data availability and the lack of comprehensive reference data, by testing the time series of various Sentinel-2 (S2) and Sentinal-1 (S1) parameters and combinations of them in order to detect mowing events in Germany in 2019. We developed a threshold-based algorithm by using information from a comprehensive reference dataset of heterogeneously managed grassland parcels in Germany, obtained by RGB cameras. The developed approach using the enhanced vegetation index (EVI) derived from S2 led to a successful mowing event detection in Germany (60.3% of mowing events detected, F1-Score = 0.64). However, events shortly before, during, or shortly after cloud gaps were missed and in regions with lower S2 orbit coverage fewer mowing events were detected. Therefore, S1-based backscatter, InSAR, and PolSAR features were investigated during S2 data gaps. From these, the PolSAR entropy detected mowing events most reliably. For a focus region, we tested an integrated approach by combining S2 and S1 parameters. This approach detected additional mowing events, but also led to many false positive events, resulting in a reduction in the F1-Score (from 0.65 of S2 to 0.61 of S2 + S1 for the focus region). According to our analysis, a majority of grasslands in Germany are only mown zero to two times (around 84%) and are probably additionally used for grazing. A small proportion is mown more often than four times (3%). Regions with a generally higher grassland mowing frequency are located in southern, south-eastern, and northern Germany.

Keywords: earth observation; remote sensing; harvests; cutting events; grazing; pasture; meadow; optical; SAR; PolSAR; InSAR

Citation: Reinermann, S.; Gessner, U.; Asam, S.; Ullmann, T.; Schucknecht, A.; Kuenzer, C. Detection of Grassland Mowing Events for Germany by Combining Sentinel-1 and Sentinel-2 Time Series. *Remote Sens.* **2022**, *14*, 1647. https://doi.org/10.3390/rs14071647

Academic Editors: Michael J. Hill and Clement Atzberger

Received: 17 January 2022
Accepted: 23 March 2022
Published: 30 March 2022

1. Introduction

Grasslands cover one third of the global terrestrial surface and fulfill multiple ecosystem functions, such as fodder production, carbon storage, provision of habitats, water

filtration, and erosion control [1–3]. In Germany, one third of the agricultural area is covered by grasslands and they are usually used to feed livestock [4] for the production of meat and dairy products. Apart from the fodder production, grasslands are important for global climate regulation as they act as carbon sinks. On land, carbon is mostly stored below ground in soils and, to a lesser extent, in vegetation. The storage capacity of carbon in soils is about 34–44% higher for grasslands than for croplands, depending on the soil depth [5]. Additionally, grasslands are potentially rich in biodiversity and they provide important habitats for plant, insect, and bird species [4,6].

In addition to site conditions, grassland functions are determined by management [7–10]. Managed grasslands in Germany are grazed and/or mown, whereby mowing is conducted one to six times per year, usually from mid-April to the end of October [4]. The frequency and timing of mowing events varies in space and time and critically influences grassland functions, such as carbon storage and biodiversity [11–13]. Usually, a more intensive use (higher mowing frequency, earlier first mowing event, more fertilizer application, higher stocking rates) of grassland leads to a negative impact on ecologically critical grassland functions, such as a decline in the species richness of plants, insects, and spiders [10,14]. Socher et al. [13] showed that species richness declined by 36% when the mowing frequency was increased from one to four times per year. The diversity in management practices and site conditions leads to a high heterogeneity of grasslands in Germany, in particular considering their species composition and fulfillment of functions. Therefore, information on the number and timing of grassland mowing events is crucial in order to monitor and model grassland functions. Furthermore, the monitoring of grasslands is required in the framework of the Common Agricultural Policy (CAP) of the European Union [15], which aims at a sustainable development of the agricultural sector in the EU.

Information on grassland management activities for individual parcels is usually not available, in particular at regional to national scales. To investigate grassland dynamics and mowing regimes at these scales, space-borne remote sensing can be applied [16]. In particular, the potential of time series from the Sentinel-2 (S2) and Sentinel-1 (S1) missions are considered high to investigate temporal vegetation patterns, as this data is available free of charge and provides high spatial coverage and resolution along with a high acquisition frequency.

Previous studies exploited space-borne multispectral optical and synthetic aperture radar (SAR) imagery to investigate grassland vegetation dynamics, such as phenology, management activities, and use intensity (for an overview see [16]). As vegetation indices based on optical sensors show a relationship to vegetation greenness and activity, it is assumed that they abruptly decrease after mowing events and increase again with vegetation regrowth. Grassland mowing events were identified by using temporal change detection methods relying on the normalized difference vegetation index (NDVI) of medium to high resolution optical data, such as Landsat 8, S2, and Formosat-2 [17–20]. Courault et al. [18] investigated Mediterranean grassland sites in France in order to model water balance and yield. The dates of mowing events, which were an important model input, were detected with Formosat-2 time series data for 120 homogeneously managed grassland parcels (all mown three times) and related well to the mowing events used for validation ($r^2 > 0.9$) [18]. Kolecka et al. [19] analyzed grassland mowing dynamics on plot scale in Switzerland with an annual time series of S2 data by detecting drops in NDVI. The results indicate that 77% of 125 mowing events on 50 validation parcels were correctly detected. Griffiths et al. [20] exploited a time series of harmonized Landsat 8 and S2 data at 30 m of ground resolution to detect mowing events for the whole of Germany, whereby the quantitative evaluation of the approach was limited by the lack of validation data. A similar approach was conducted by Schwieder et al. [17] as they used the enhanced vegetation index (EVI) derived from Landsat 8 and S2 data to detect mowing events with dynamic thresholds and a rule set. This approach was tested for around 90 parcels with 214 mowing events and led to an average F1-Score of 0.61 for an allowed time difference of 15 days between detected and observed mowing events [17]. The latter approaches highlight that investigating all of the

grasslands in Germany via remote sensing time series analyses leads to challenges and difficulties due to the heterogenous nature and diverse management practice of grasslands. The limitation of optical data to cloud-free scenes [19] and the lack of an independent reference dataset [20] were identified as the major drawbacks by the studies.

Previous studies based on SAR data used the temporal evolution of the backscatter, interferometric (InSAR) and polarimetric (PolSAR) features to analyze grassland mowing dynamics. Some studies showed that mowing events in German grassland sites led to changes (peaks) in the S1 backscatter time series [21,22]. This effect is probably based on the increase in reflectance from soil due to the shorter grass after the mowing event. Taravat et al. [23] detected grassland mowing events for 10 grassland parcels in Bavaria, Germany, with an overall user's accuracy of 85.7% (six of eight mowing events were detected) using a classification approach based on deep learning and S1 backscatter data. On the contrary, other research revealed inconsistent patterns of SAR backscatter behavior after mowing events of grasslands in Estonia and Belgium [24,25] or found no significant relationship to biophysical parameters, such as vegetation height and biomass [26,27]. Signals of InSAR temporal coherence were studied before, during, and after mowing events of grassland sites in Estonia, based on Cosmo-Skymed [26,27], TerraSAR-X [25,28,29], and Sentinel-1 [30,31] time series to investigate the potential of using it as feature for grassland mowing detection. The theoretical assumption is that the coherence is higher after a mowing event than before when both images are from after the event, as the images are more correlated due to less motion and more similar physical properties of short grass than long grass [31]. In general, relationships to management activities or biophysical parameters were found [26,27], but patterns were unclear in space and time and as such the value of including InSAR features was limited [29,30]. Recently, De Vroey et al. [24] detected mowing events based on temporal InSAR coherence time series of S1 for grassland sites in southern Belgium. Around 56% of the mowing events were successfully detected with this approach, pointing to a potential of InSAR coherence to detect management activities. Furthermore, [25,28] investigated PolSAR decomposition features of TerraSAR-X and Radarsat-2. The authors found relationships but no direct correlations between some decomposition parameters and the grassland mowing regime.

Apart from synergistic investigations, such as visual inspections and correlations of S1 and S2 time series over grasslands [31,32], only Lobert et al. [33] combined optical and SAR data to detect mowing events, to the best of our knowledge. By using a one-dimensional convolutional neural network, mowing events were detected with a classification approach for three regions in Germany. The combination of NDVI, backscatter cross-ratio and InSAR coherence led to the best modelling results (F1-Score of 0.84) when a deviation of 12 days between the detected and actual mowing event was allowed. The major drawback of the study was the lack of a comprehensive reference dataset (64 parcels and 257 mowing events in three years), as the mowing information was only available for parcels that were mown up to four times, with most parcels only mown one to two times [33].

The few studies that investigated the potential to map grassland mowing events with satellite data beyond plot scale focused solely on optical datasets [17,19,20] and are therefore limited by clouds. In addition, previous studies lack sufficient reference data, which should include grasslands with a complete range of mowing frequencies in the studied area. In this study, we investigated the parameters of optical and SAR sensors in order to develop a mowing detection algorithm based on observations of a parametrization dataset, instead of theoretical assumptions, such as those largely conducted in previous studies. We combined information from S1 and S2 to detect and analyze the grassland mowing regime for the whole of Germany at high spatial resolution of 10–20 m. Time series of various S1 and S2 parameters from the vegetation period (March to November) 2019 were tested in order to design an algorithm for gap-free mowing detection. The reference dataset used for parametrization and validation of the mowing detection algorithm was a comprehensive and independent dataset consisting of daily images, depicted from webcams and self-installed cameras at grassland sites all over Germany. Based on the developed algorithm,

we created three main products, such as the mowing frequency, the dates of single mowing events, the date of the critical first mowing event, and two quality layers for Germany.

2. Materials

2.1. Study Area

2.1.1. Germany

This study covers grasslands in Germany, which occur throughout the country. Areas covered by grasslands are especially widespread in the north-west and in the south (Figure 1A). Grasslands often appear in regions that are unsuitable for crop growth, either due to unfavorable climatic or site conditions, leading to a widespread grassland occurrence in high altitudes, on steep slopes, or in areas with poor or wet soils [4]. Grassland parcels are relatively small compared to other agricultural parcels, whereby 25% are smaller than 1.3 hectares and 50% have less than 2.9 hectares [4]. They occur on different altitudes and moisture gradients and vary strongly in their plant species composition. Grasslands are potentially rich in plant species and are characterized by plants with successive flowering periods [34]. The plant species richness and the dominance of single species is determined by the management regime and site conditions and, therefore, varies strongly across Germany [34]. The same applies for grassland yields; however, the standing biomass usually peaks at the beginning of June [35]. Grasslands in Germany are mainly mown and/or grazed and are regularly fertilized [4]. The timing and frequency of these management activities vary strongly, and the mowing frequency ranges between one and six times per year. An annual mowing frequency of one to two times is considered as extensive management, three times as moderate, and four to six times as intensive [4]. After the mowing event, the vegetation is at times left on the parcel to dry for several days.

The Copernicus grassland high resolution layer (HRL) of 2018 [36] at 10 m resolution, (overall accuracy was 89.9%), was used to mask areas not covered by grasslands. The HRL includes all grasslands (natural/semi-natural) and is based on a classification with S1 and S2 data. The mowing detection approach of this study is applied to all HRL grasslands in Germany, as natural grasslands are potentially also mown for maintenance.

2.1.2. Focus Region

A relatively high number of reference data was available for the Ammer region (Figure 1B), which is a focus region of the SUSALPS project (https://www.susalps.de/en/, accessed on 25 March 2022). This region is characterized by humid continental climate, according to the Koeppen–Geiger classification [37], with a wide range in sub-climates due to an altitudinal gradient (580–2050 m a.s.l.). The occurring grasslands are pre-alpine and alpine and are widely distributed (around 90% of agricultural area) in the focus region. They show a broad range of management types (mown vs. grazed or a combination of both) and intensities (e.g., zero to six mowing events per year). Therefore, grassland parcels from the focus region are used to develop and parameterize the satellite-based mowing event detection. In addition, the focus region is used to analyze the potential of a combined mowing event detection based on optical and SAR data.

Three exemplary grassland parcels were picked from the focus region to show investigated parameters for all satellite data types used in this study (Section 3.2.1, Table S1, Figures 1B and 3). These three grassland sites are characterized by relatively similar climatic conditions (Table S1, [38]) but differ in their mowing frequency, which is three, four, and five times per year.

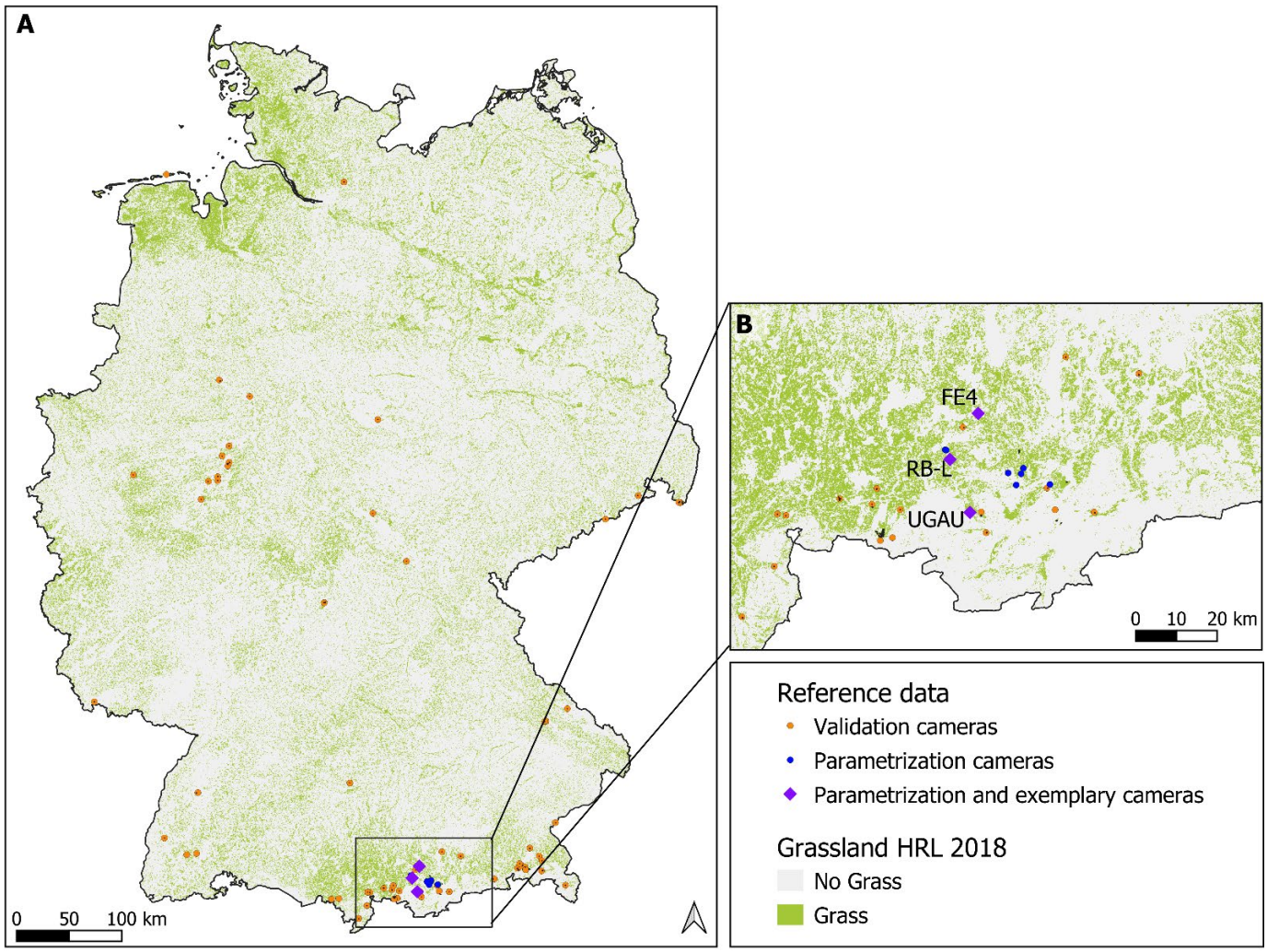

Figure 1. Distribution of grassland in Germany (**A**) and the focus region (**B**) according to the Copernicus grassland HRL for 2018 [36], and camera positions used to derive information on mowing dynamics to parameterize and validate the satellite-based products.

2.2. Ground Data

Daily information from 80 cameras from the year 2019 was used to parameterize and validate the detection of grassland mowing events with satellite data. The cameras distributed over Germany (Figure 1A) consisted of 69 public webcams (Table S2, Figure S3) and 11 cameras, which were installed at grassland sites of cooperating farmers. All cameras took at least daily RGB images, and several had a field of view that covered multiple (up to eight) grassland parcels, so that reference information of overall 192 parcels was available. These parcels and their location were determined by inspection of the webcam location, the image field of view and high-resolution satellite products (e.g., Google Earth). Based on this, grassland parcel polygons were created, which were further used to extract the satellite data at each grassland parcel location. The pictures taken by the cameras allowed us to gather information on management activities, such as the timing of the mowing events and the presence of grazing animals. The daily RGB images from the cameras were visually evaluated and mowing events were noted. This was conducted by looking at every camera image per day and noting down each management activity on each grassland parcel. In total, 536 mowing events were registered, which were used for parametrization (n = 45) and validation (n = 491).

2.2.1. Parametrization Data

To develop the mowing detection approach, time series of 13 parametrization sites from the focus region were examined (Figure 1B). These reference sites show a high variety in management activities and differ in their water availability, species richness, and appearance. Mowing frequencies on these parcels range from one to six events per year, some are fertilized, and some parcels are additionally grazed (Table S4). The 13 differently managed grassland parcels, recorded from nine cameras, resulted in 45 mowing events, which were used to investigate satellite data time series and parameterize the thresholds to detect mowing events. Data from these reference parcels were excluded from validation.

2.2.2. Validation Data for National Mowing Event Detection

Apart from the 13 parametrization reference sites, 179 grassland parcels in Germany were available to validate the developed mowing detection algorithm based on S2 (Figure 1A). The visual examination of camera RGB images of these grasslands resulted in 491 registered mowing events. Almost 50% of these grasslands were mown three to four times per year, more than 40% one to two times, and 10% showed more than four mowing events per year. However, due to technical problems or cloudy weather conditions, the continuous derivation of management information was limited for about half of the cameras, resulting in 89 grassland parcels with gap-less RGB image-based validation information and 283 mowing events, in total. The remaining 90 grassland parcels affected by these problems were excluded from the validation of the mowing frequency (Section 3.2.2).

2.2.3. Validation Data for the Mowing Event Detection in the Focus Region

The focus region includes a subset of the cameras across Germany, resulting in recordings from 66 grassland parcels with, in total, 229 mowing events for validation that were not used for parametrization (Figure 1B). All of these cameras acquired continuous daily images. These data are used to validate the combined approach using S2 and S1 data (Section 4.4, [39]). Validation statistics of the combined approach are compared to those derived from using only S2 data to detect mowing events in the focus region.

2.3. Satellite Data

S1 and S2 time series data from Copernicus, which are freely accessible, were analyzed in this study. The S2 fleet consists of two satellites (S2-A and S2-B) with identical optical, multi-spectral sensors, acquiring information in 12 bands [40]. The spatial resolutions of these bands are 10, 20, and 60 m. The combination of S2-A and S2-B allows for a revisit time (in Germany) between two and five days. Data of all 63 S2 tiles covering Germany were processed from March to November 2019 (Figure 2), resulting in 3465 datasets, which were processed. The northern hemispheric winter months, December to February, are not included as the vegetation is inactive during this period. Due to partly overlapping S2 orbits, the data coverage is not homogeneous for Germany (Figure 2). In addition, optical data is limited by the availability of cloud-free scenes.

S1 consists of two polar-orbiting satellites (S1-A and S1-B) with identical SAR sensors, acquiring information in C-band [41]. Radar data acquisition is independent from day-light and atmospheric conditions. In this study, the ground-range-detected (GRD) products were used to analyze the backscatter intensity information. In addition, based on the single-look-complex (SLC) data, interferometric coherence (InSAR), and polarimetric decomposition (PolSAR) parameters were calculated. The repeat cycle of S1 is six days as data from both satellites (S1-A and S1-B) were included. All S1 products were acquired in the interferometric wide-swath mode (IW) and in dual polarization (VV/VH). Data from March to November 2019 was processed for RON 117 in ascending mode as backscatter and InSAR and PolSAR features were exclusively tested for the focus area of the Ammer region, resulting in 90 processed S1 datasets (45 S1 GRD, 45 S1 SLC).

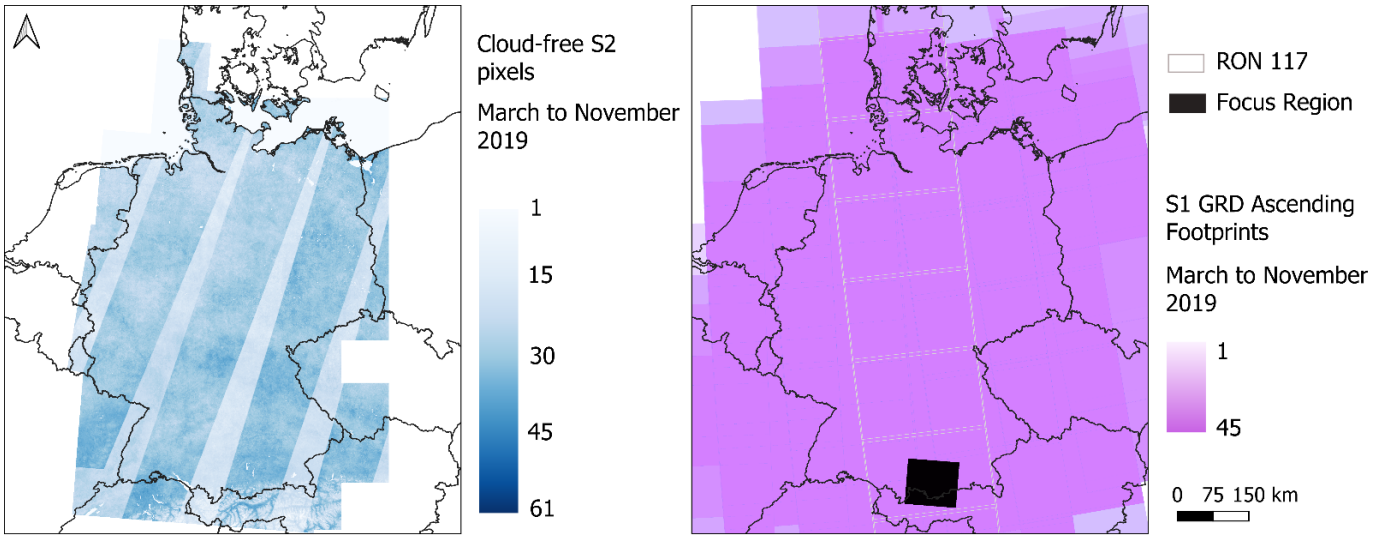

Figure 2. Data coverage of S2 after cloud screening and S1 for the period: 1 March 2019 to 30 November 2019 cropped to Germany, highlighting the inhomogeneity in data distribution due to overlapping orbits and varying cloud coverage of S2.

3. Methods

To analyze the potential of several S1- and S2-based parameters to detect mowing events, time series of these were pre-processed and their temporal profiles and reactions to mowing events were examined. The most suitable parameters were selected according to their relative changes after mowing events and the mowing detection approach was developed and parameterized. The approach based on S2 only was used to detect and validate mowing events across Germany and the combined approach of S1 and S2 was tested for the focus region.

3.1. Pre-Processing of Satellite Data

3.1.1. Pre-Processing of Sentinel-2 Data

Pre-processed surface reflectance data and cloud information calculated with the MAJA algorithm (version 3.3) [42] was used. Cloud screening of the S2 surface reflectance data was performed by excluding pixels with clouds, cloud shadows, and topographical shadows, as detected by the MAJA algorithm. This algorithm showed a relatively strict cloud detection, which was desired here as clouds and cloud-effects are easily confused with mowing events. In addition, all scenes were masked with the Copernicus HRL grassland 2018 [36] and only the pixels that represent grassland were retained. The near-infrared (NIR, central wavelength = 832.8 nm), red (central wavelength = 664.6 nm), and blue (central wavelength = 492.4 nm) bands, all in 10 m spatial resolution, were used for vegetation index calculations. The enhanced vegetation index (EVI) was calculated for each valid scene with the following formula [43]:

$$\mathrm{EVI} = 2.5 * \frac{\mathrm{NIR} - \mathrm{RED}}{\mathrm{NIR} + 6 * \mathrm{RED} - 7.5 * \mathrm{BLUE} + 1} \quad (1)$$

The resulting S2 EVI layers were then assembled to a time series to analyze the temporal evolution of the EVI per pixel. The EVI time series were filtered, interpolated, and smoothed as follows: First, negative EVI values and values above two were filtered, as those are usually not associated with vegetated land and can be assumed as outliers. Each time series produced at pixel level was afterwards linearly interpolated to obtain a daily continuous time series. These time series were smoothed with a Savitzky–Golay filter [44], with a window length of 31 days and a polynomial fit of order two, to minimize small fluctuations.

3.1.2. Pre-Processing of Sentinel-1 Data

Time series of S1 were processed twofold. First, just using the intensity information, GRD images were processed by the application of the most recent orbit files, removal of border noise and thermal noise, and radiometric parametrization. A refined Lee speckle-filter was applied with a window size of 3 × 3. The SAR data was corrected using the EU-DEM [45] and resampled to a spatial resolution of 10 m. Prior to the analysis, VV and VH intensities were transformed to gamma nought and to logarithmic scale (dB).

Second, single-look-complex (SLC) imagery was downloaded for the focus area of the Ammer region. After the application of the orbit files and the parametrization, polarimetric features of the dual-polarization entropy/alpha decomposition were processed by deducing the covariance matrix (C2) and the VV/VH-polarized Kennaugh matrix [46–48]. The PolSAR entropy informs on the degree of scattering randomness (i.e., depolarization) and ranges between zero and one. Higher values are related to higher degrees of randomness/depolarization and vice versa [48]. The investigated Kennaugh matrix parameter K0 is a measure of the total intensity (span) of VV and VH, whereas K1 is a measure for the difference between VV and VH. Kennaugh elements K5 and K6 describe the real and imaginary part of the signal, but were not included in the analysis due to their limited value in characterizing land surface properties, in particular vegetation dynamics [49].

Besides, the interferometric coherence was estimated for both channels following the processing strategy developed in preliminary work [50]. The InSAR coherence is a measure for correlation of two complex SAR signals. It ranges from zero to one, whereas zero means complete decorrelation and one perfect correlation. The InSAR coherence is affected by several types of decorrelation [51], of which the temporal correlation is of main interest for this study as it inherits information on temporal changes in the position and physical properties of scatters between both images [51–53] and as such might provide information on grassland mowing events.

The time series of all SAR features (i.e., VV and VH intensities, K0, K1, entropy, VV, and VH InSAR coherence) were smoothed using a Savitzky–Golay filter [44]. Various parameters for the smoothing were tested and a rather strict setting with a window size of 31 days and a polynomial fit of order two was applied. In addition, the data was masked with the grassland HRL 2018 [36] to exclude areas not covered by grassland.

3.2. Mowing Detection Approach Development

To develop the grassland mowing detection approach, time series of 13 parametrization sites were analyzed. All investigated optical and SAR variables were investigated regarding their reaction after mowing events. In addition, the averaged values before all mowing events (n = 45) were compared to the averaged values afterwards. Based on this, the most suitable variables for detecting mowing events were selected and the detection rule-set was created empirically. To determine the optimal thresholds for the detection approach, initial values were set according to the observations made while investigating the time series and the averaged changes after mowing events. Multiple values around these initial thresholds were tested regarding their potential to detect mowing events. The final thresholds were selected according to the highest accuracies achieved (Section 3.3.2).

3.2.1. Investigation of Satellite Time Series and Variable Selection

Time series of S2 and S1 features for the 13 parametrization parcels of the Ammer region were investigated to examine their temporal behavior in relation to mowing events. For all calculated parameters (i.e., EVI, backscatter VV, backscatter VH, InSAR coherence VV, InSAR coherence VH, PolSAR entropy, K0, K1) the center-pixel of the parcel, a 3 × 3 window-average around the center pixel, and the parcel-based average time series were visually examined. There were only marginal differences between these three types of time series for all parameters and all 13 parcels (not shown). Thus, only the center-pixel-based data are further examined.

Figure 3 shows the center-pixel time series of four parameters (one of each satellite data category), including mowing dates (reference data), presence of cows, and large data gaps of the optical time series (>25 days) for the three selected exemplary parcels (Supplementary SI). The remaining parameters are not shown as the information is redundant. Raw and smoothed values are shown to highlight the effect of smoothing, which is needed to detect mowing events with the approach presented here. The three parcels were mown five (RB-L), four (FE4), and three times (UGAU) in 2019. To examine the effect of soil moisture, especially on the SAR-based parameters, precipitation recorded by climate stations within a distance of less than 3 km are additionally shown as weekly sums. The visual examination of the time series of S2- and S1-based parameters (Figure 3) revealed that particularly the EVI time series shows reliable, strong drops in most cases after grassland is mown. Some events were missed or were less strong (e.g., third event RB-L, third event FE4, second event UGAU), which might be related to cloudy periods (Figure 3, blue bars). Considering the SAR features, backscatter VV shows only a marginal relationship to the mowing events. PolSAR entropy and InSAR coherence VV reveal peaks after mowing event which, however, were less pronounced and less consistent than the reactions visible in the EVI temporal signal.

To quantify the change in the remote sensing signals induced by a mowing event, and hence to select the most suitable parameters to develop the detection approach, the raw and interpolated/smoothed values before and after all mowing events of the 13 parametrization sites (n = 45) of each parameter were plotted (Figure 4). Values of six days before and six days after each mowing event of all mowing events were summarized as boxplots (Figure 4). In addition, the absolute differences between the six-day periods before and after a mowing event averaged over all mowing events (n = 45) were normalized with the 95% percentile of each parameter of the value distributions (raw and smoothed) of the parametrization sites to make the differences comparable among the various parameters (Table 1). Due to clouds, the raw EVI potentially has less data points than the interpolated and smoothed EVI and the other parameters. The EVI shows the strongest reaction, namely a drop of 0.25 for the raw data and 0.09 for the smoothed data on average after the mowing event when the means are compared (Figure 4, Table 1). The entropy shows an increase of 0.04 (normed) after mowing events (Table 1). K1 is inversely related to the entropy and shows weaker effects after mowing events (Figure 4, Table 1). In addition, the entropy should be preferred as it has a defined value range in contrast to K1. K0 and backscatter VV show almost no reaction and the increase in backscatter VH is only marginal (Figure 4, Table 1). Both coherence VV and coherence VH show—on average—an increase after mowing events in a similar range as PolSAR entropy (Table 1); however, because the coherence values are all very low (<0.4) and around the noise level, entropy is preferable (Figure 4). The EVI was selected as the main parameter for the mowing event detection. Besides the EVI time series, the entropy seems to be most useful regarding its potential to detect grassland mowing dynamics (Figures 3 and 4, Table 1).

Table 1. Average absolute differences of six days before and six days after a mowing event for all mowing events (n = 45) of all 13 parametrization sites. The differences are normalized with the 95% percentile of each parameter of all values of the parametrization sites of raw and smoothed data, accordingly.

	EVI	ENT	K0	K1	BS VV	BS VH	COH VV	COH VH
Normalized difference (Raw data)	0.29	0.14	0.002	0.06	0.03	0.08	0.08	0.09
Normalized difference (Smoothed data)	0.11	0.06	0.0009	0.02	0.008	0.02	0.06	0.06

EVI = Enhanced vegetation index, ENT = PolSAR entropy, K0 = PolSAR K0, K1 = PolSAR K1, BS VV = Backscatter VV, BS VH = Backscatter VH, COH VV = InSAR coherence VV, COH VH = InSAR coherence VH.

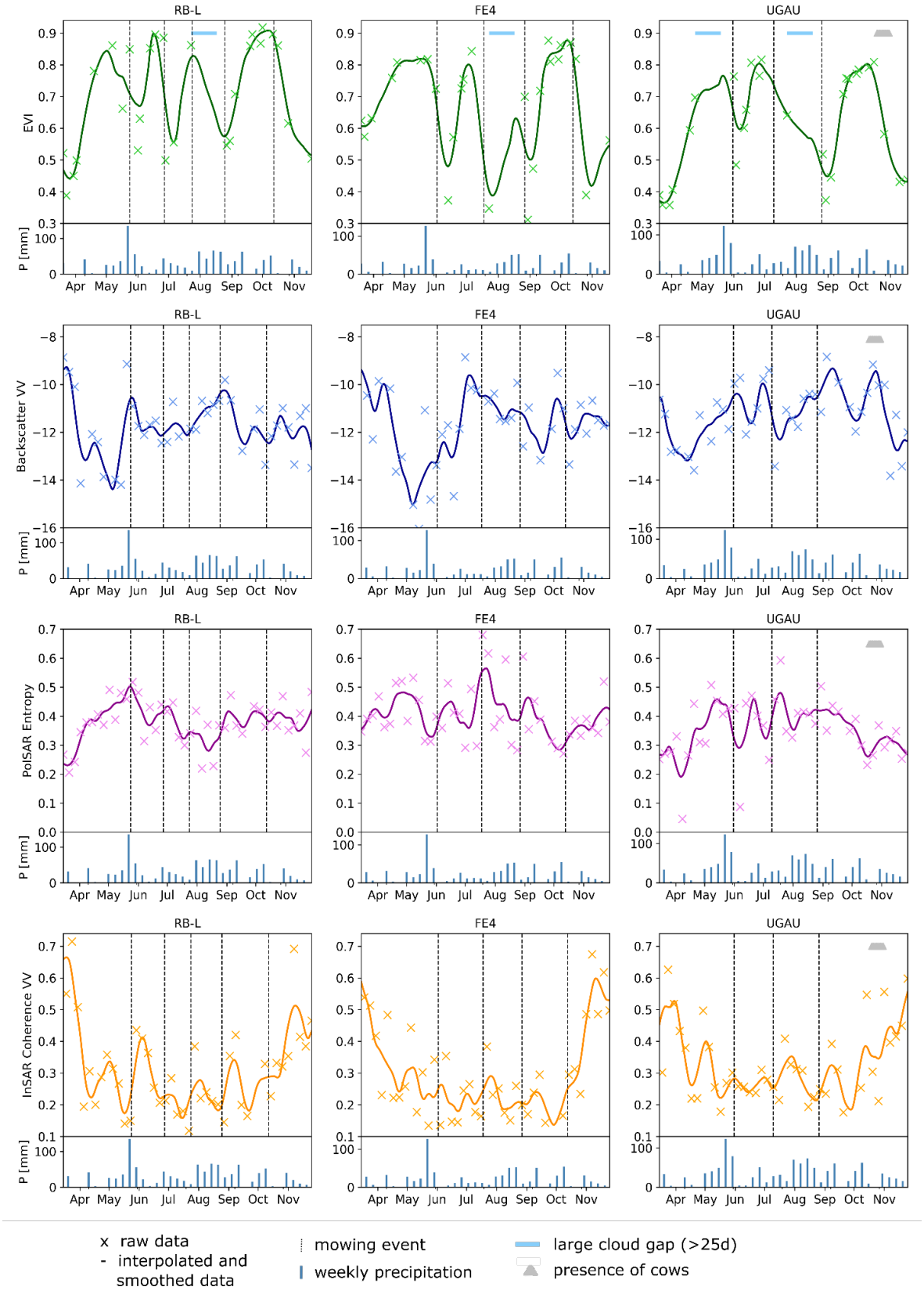

Figure 3. Time series of S2- and S1-based parameters for five (RB-L), four (FE4), and three (UGAU) times mown grassland parcels, including information on the mowing date (vertical lines), presence of cows, and large data gaps (>25 days) within the optical time series and weekly precipitation sums (bottom plots).

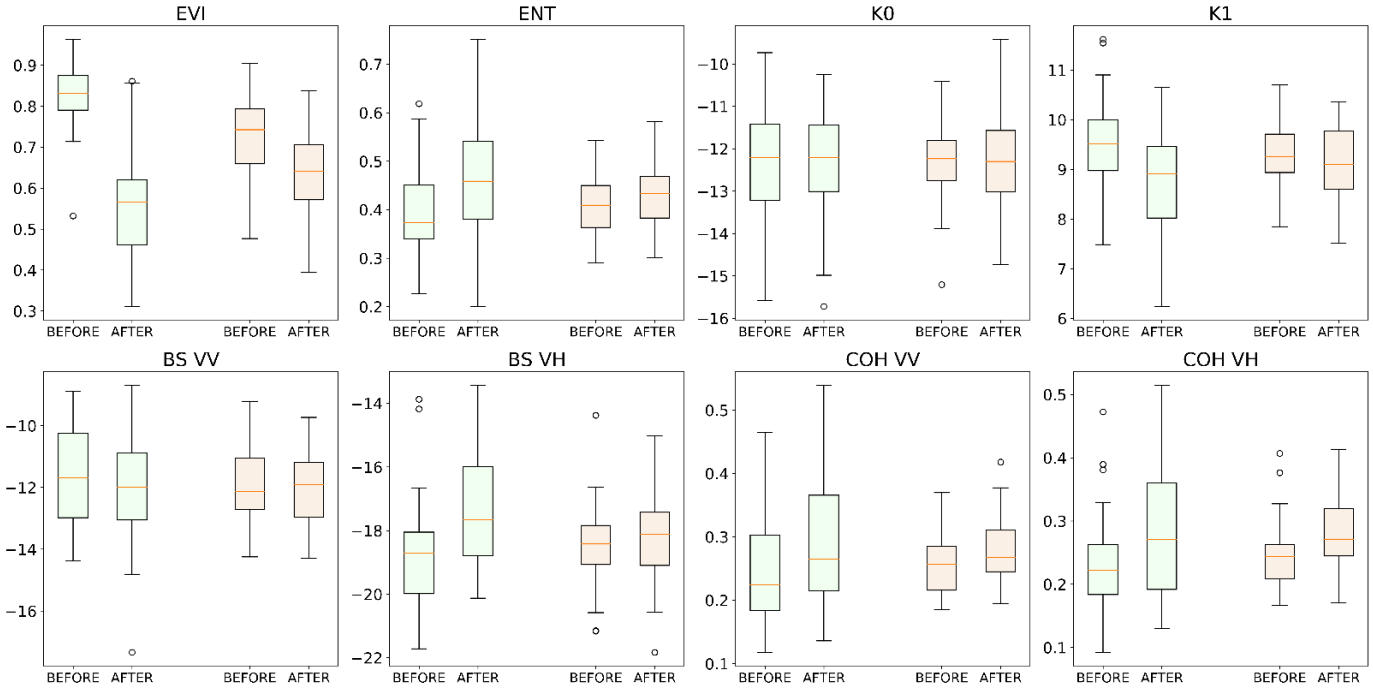

Figure 4. Data values of observed parameters for a period of six days before and six days after a mowing event for all mowing events (n = 45) of all 13 parametrization sites. Left: raw data (green boxes. Right: interpolated and smoothed data (orange boxes).

3.2.2. Rule-Set Development and Parametrization

The investigation of the time series of the reference sites (Figures 3 and 4, Table 1) revealed clearly that the EVI is the most suitable parameter to detect grassland mowing events as strong decreases were visible in the time series after mowing events. However, these drops were at times not present, which was often related to missing data due to clouds (more detail in Section 4.1). Therefore, a second mowing event detection algorithm was developed and tested, which includes the PolSAR entropy as second parameter. Within the combined approach (EVI + Entropy), mowing events were detected according to the EVI time series when valid EVI observations were available; in the case of prolonged times of missing observations, the detection using the PolSAR entropy was conducted.

EVI-Based Mowing Detection Algorithm

The examination of the EVI time series of the 13 parametrization sites show a strong and abrupt decrease in EVI at mowing events, followed by a subsequent increase. Based on these observations (Figures 3 and 4, Table 1), the detection of mowing events via the EVI was derived as follows: (i) The local minima within the pixel-based EVI time series for the growing season are localized. (ii) The EVI of the local minimum is compared to the EVI of the previous peak (i.e., local maxima). (iii) To successfully detect a mowing event, the amplitude of EVI between these two extrema needs to exceed a threshold 0.07 (th_1). (iv) An immediate EVI increase of at least +0.02 (th_2) has to follow the local minimum as additional condition for the mowing detection. The values for the thresholds th_1 and th_2 were determined according to the best accuracy achieved (see Section 3.3.2), whereby for th_1 a range from 0.1 to 0.15 and for th_2 a range from 0 to 0.05 was tested with steps of 0.01.

When these conditions (i–iv) are fulfilled, a mowing event is detected, and the date of the event is defined as the average date between the detected local minimum and the previous maximum. Even though the event could have happened within the entire period (i.e., between the dates of the local minimum and previous local maximum), the offset in detection is minimized on average.

EVI + Entropy-Based Mowing Detection

Although the EVI was determined to be the most suitable parameter to detect mowing events, some events might be missed due to clouds. Therefore, a SAR-based parameter was used to support the mowing detection when the EVI-based detection might fail due to cloudy conditions. The visual examination of the PolSAR entropy time series showed a relationship to the mowing regime (i.e., entropy maxima after mowing (Figures 3 and 4, Table 1)). However, this pattern was less consistent and less reliable compared to the EVI change after a mowing event. Therefore, the temporal evolution of the PolSAR entropy signal is only considered for mowing detection when large gaps of the optical time series are present. These gaps are defined as being at least 25 days long. The following procedure was developed to detect additional mowing events with EVI and PolSAR entropy time series: (i) When a large gap in S2 data is present, the PolSAR entropy time series of five days before the gap until 10 days after the end of the gap (resulting in at least 40 days) is analyzed for peaks. (ii) The shortened PolSAR entropy time series is inspected for local maxima, which is then compared to the previous local minimum or, if no local minimum is present, to the global minimum of the shortened time series. (iii) The magnitude between these values needs to exceed a threshold of 0.05 (th_3). The value for th_3 was initially set by observations made while investigating the parametrization sites (Figures 3 and 4, Table 1). The final value of th_3 was defined by determining the best accuracy for the detection approach by checking F1-scores (Section 3.3.2) with the parametrization sites, whereby a range from 0.03 to 0.1 was tested. When the condition is met, the mowing event is defined as the average date between the local minimum and the local maximum. (iv) Finally, the PolSAR entropy-based detections are compared to the EVI-based detections, and only when they were missed, they were registered as additional mowing events. The allowed time difference between the S1-based and the S2-based approach in that regard was 10 days or less.

3.3. Validation Procedure

3.3.1. Validation Procedure for the Detection of Grassland Mowing Events

To examine whether mowing events were correctly detected by the satellite data-based approach, the detected dates were compared to the validation dataset. The majority of the detected mowing dates per parcel were combined for each mowing event to make them comparable to the validation data that was on parcel level. A difference of up to seven days between the detected and the actual mowing event date was accepted for a correct detection. In addition, falsely detected mowing events by the satellite-based approach were registered.

3.3.2. Accuracy Assessment of the Mowing Event Detection

Next to the percentage of correctly detected mowing events, the F1-Score was calculated to evaluate the mowing detection approach, which is an adequate measure for imbalanced classes [39], as follows:

$$F1 = 2 * \frac{\text{precision} * \text{recall}}{\text{precision} + \text{recall}} = \frac{TP}{TP + \frac{1}{2}(FP + FN)} \quad (2)$$

where precision is a measure of exactness and recall of completeness, TP is the number of true positives, FP the number of false positives, and FN the number of false negatives. To calculate the precision, the number of false positives is needed. Only grasslands (n = 89) for which the exact mowing frequency could be depicted through the availability of gap-less RGB images were included in the validation of mowing frequency and the F1-Score (see Section 2.2.2).

3.4. Uncertainty Information

An indicator for the availability of the S2 time series was derived by quantifying large gaps (>25 days) within the EVI series. These gaps, which are usually induced by clouds, were summed up and the spatial patterns were compared to the S2 only and the S1 and S2 combined detected mowing events.

In addition to this quality indicator derived from the S2 data availability, an indicator for the uncertainty of each individual mowing detection based on S2 data was developed. This indicator is composed of two parameters derived from each S2-based mowing event detection, as follows: (i) The first parameter is defined as the data availability before and after the event and (ii) the second parameter as the magnitude of the EVI amplitude during a mowing event detection. The data availability around a detected mowing event (i) was thereby determined by locating the last valid S2 scene before and the first one after the event. The resulting time span ranged from two to several days with a maximum of around 100 days. The lower the time span, the more the mowing event detection relied on measured S2 data, and not on interpolated EVI values, increasing the detection reliability. The second aspect of the uncertainty analysis was the magnitude of EVI decrease (ii) resulting in a mowing detection. For each event, the gradients were calculated as the difference in smoothed EVI values between the local maximum and minimum divided by the time period between the local maximum and minimum. To adjust the gradients to the first uncertainty measure—the data availability—they were multiplied by 10,000. After this operation, the gradients (ii) ranged between 10 and around 300 and were therefore three times larger than the data availability measure (i). The higher the gradient, the stronger the local minimum in a shorter time, and the more certain the mowing event detection. To derive a combined uncertainty, the data availability time spans (i) were subtracted from the gradients (ii). This way, the importance of the EVI gradients was weighted 3 times higher than the data availability time spans as the value range of the EVI gradients was three times higher than the data availability information. The combined uncertainty was divided by 300 to range around 0, with a range of [–2, 2]. The lower the value, the more certain the mowing event and vice versa. This uncertainty information is averaged over all mowing events to estimate an overall uncertainty for the detected mowing frequency.

4. Results

4.1. Accuracy Assessment on Parametrization Sites

4.1.1. EVI-Based Mowing Detection Algorithm

The EVI time series of the parametrization sites showed a strong relationship to the mowing regime (Figure 5). When applying the EVI-based mowing event detection approach to the 13 parametrization sites, 34 of the 44 mowing events were successfully detected if a time difference of seven days between the date of detection and the actual mowing date was allowed. Ten events were missed, and 10 dates were falsely detected as mowing events, resulting in an F1-Score of 0.77. The amplitude of the EVI thresholds had only minimal effects on this result as the F1-Scores remained the same for values of 0.02 to 0.12 for the first (th_1) and values of 0 to 0.04 for the second threshold (th_2). The mowing detection approach based on EVI also lead to falsely detected mowing events due to grazing activity (i.e., HF). The drop in EVI after mowing only lasted for around 10 to 14 days, highlighting that dense optical time series are crucial in order to successfully detect mowing events.

While inspecting the time series of the parametrization sites (Figure 5), it becomes obvious that mowing events were missed by the EVI only approach when there was no EVI information available within the gaps induced by cloud coverage. Mowing events were missed or the detected dates were not completely correct during, shortly before, or shortly after cloudy periods, as local minima were not recognized (i.e., 3rd and 4th event RB-L, 2nd event UGAU, 4th event GL, 3rd event MN, and 3rd event RB1, 4th event FE2). Of the 10 missed mowing events of the parametrization dataset, eight were within cloud gaps or shortly before or after.

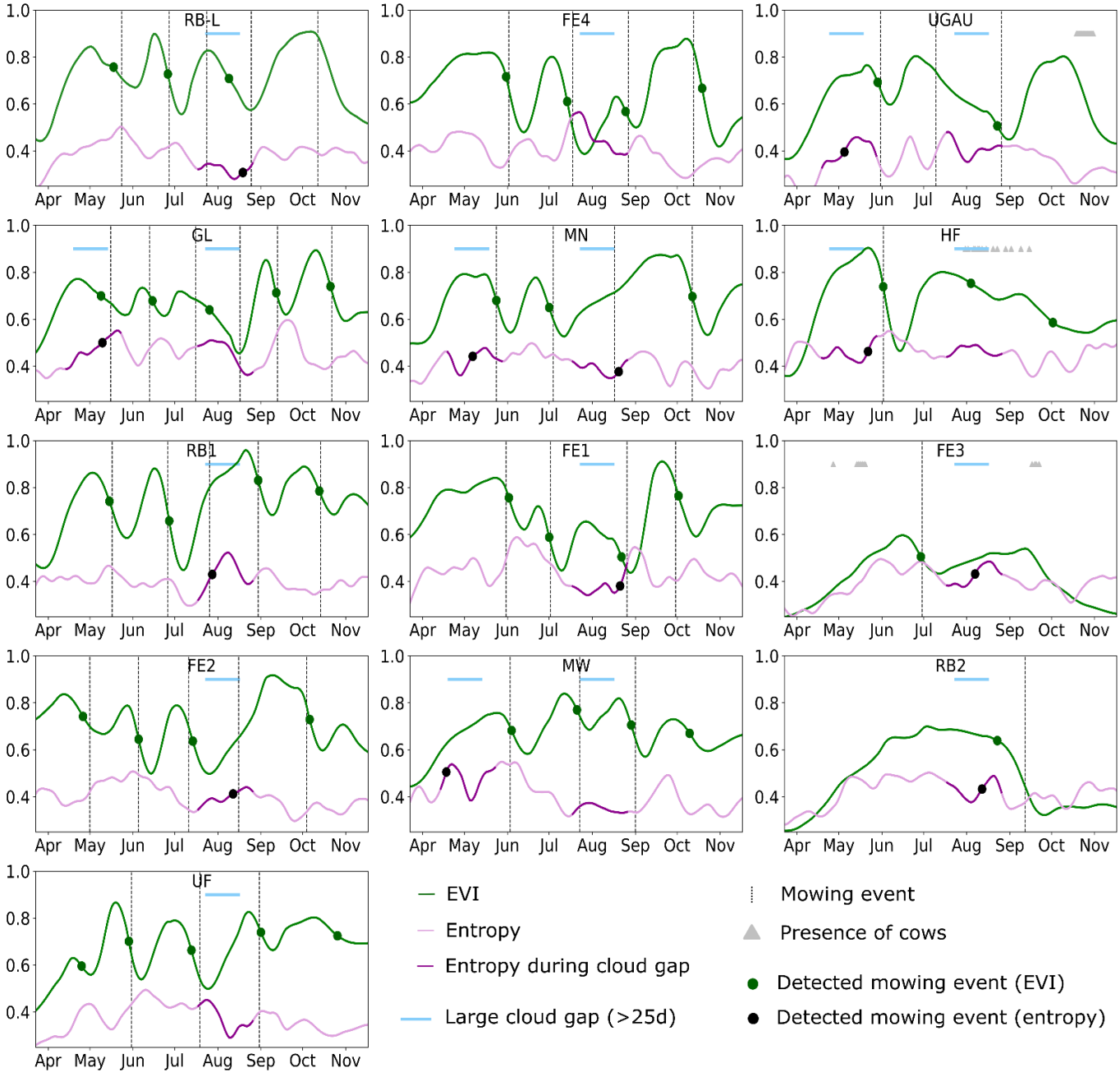

Figure 5. Temporal profiles of gap-filled and smoothed EVI and PolSAR entropy for center pixels of the parametrization grassland parcels with varying mowing regimes, including the actual and detected mowing events as well as gaps within the optical series.

4.1.2. EVI + Entropy-Based Mowing Detection

The detection of mowing events based on peaks in PolSAR entropy within long gaps of optical data (>25 days) lead to 12 mowing event detections (Figure 5), of which eight were correct. Of these, five were already detected as mowing events by the S2-based approach (3rd event FE1, 1st event GL, 1st event HF, 1st event RB2, 4th event RB-L). The detection on the RB-L site was actually not correct based on S2, but the algorithm would not count the S1 detection as new because it is too close to the S2 detection ($\leq$10 days). Within the parametrization dataset, three additional S1-based detections were correct, which were missed using the EVI-only approach (4th event FE2, 3rd event MN, 3rd event RB1). In addition, four falsely detected mowing events occurred (FE3, UGAU, MN, MW).

Hence, for the parametrization dataset (Figure 5), the integration of the PolSAR entropy-based detection increased the amount of detected mowing events by three and added four false positives (84.4% successful detections, F1-Score = 0.78) compared to the case when only the EVI-based detection was applied. The tests with different PolSAR entropy thresholds revealed a high sensitivity to the number of detections, as such steps showed that weaker smoothing or smaller thresholds of the entropy increased the number of false positives rapidly.

4.2. Mowing Detection Validation of the Focus Region

From the total of 229 mowing events located in the focus region (Figure 1B), 148 were correctly detected (64.6%) by applying the S2-based mowing detection approach and with an allowed difference between detection and actual event of seven days. By complementing the detection approach with the analysis of PolSAR entropy time series within larger cloud gaps of optical data (>25 days) in the focus region, the detection of mowing events was improved by detecting an additional 21 mowing events to 73.8% of correctly detected events. The number of false positives increased strongly from 76 to 157 falsely detected mowing events (Table 2) when the PolSAR entropy-based detection was applied. The F1-Score for the focus region within the Ammer region was 0.65 when the S2 only-approach is used and dropped to 0.61 when the combined S2 and S1 approach is used.

Table 2. Accuracy matrix of detected mowing events showing successfully detected, missed events, and false positives for the focal region in the Ammer catchment area.

		Actual Condition (Validation)	
		Mown	**Not Mown**
Predicted Condition (Satellite-based detection) S2 only	Mown	148	76
	Not mown	81	
Total		229	
Predicted Condition (Satellite-based detection) S2 + S1	Mown	169	157
	Not mown	60	
Total		229	

When comparing the actual (true) distribution of mowing frequencies among the grassland parcels in the focus region with the detected frequencies by S2 only and the combined approach, it becomes clear that using only EVI leads to an underestimation and EVI plus PolSAR entropy to an overestimation of the mowing frequency (Figure 6). The spatial pattern of the combined approach (Figure 7) reveals that adding the PolSAR entropy-based detection to the EVI-based approach could not balance the systematic lower number of detected mowing events in regions with lower S2 orbit coverage by the S2-only approach (compare Figure 2).

4.3. Germany-Wide Validation of S2-Based Mowing Detection

From the total of 491 mowing events on validation parcels distributed all over Germany, 60.3% were successfully detected with the S2-only approach (i.e., just using the EVI-based detection), when the allowed time difference between detected and actual mowing date was seven days. The influence of the allowed time difference on the detection success is visualized in Figure 8. The time difference between the actual and the detected mowing event was, on average, 2.5 days.

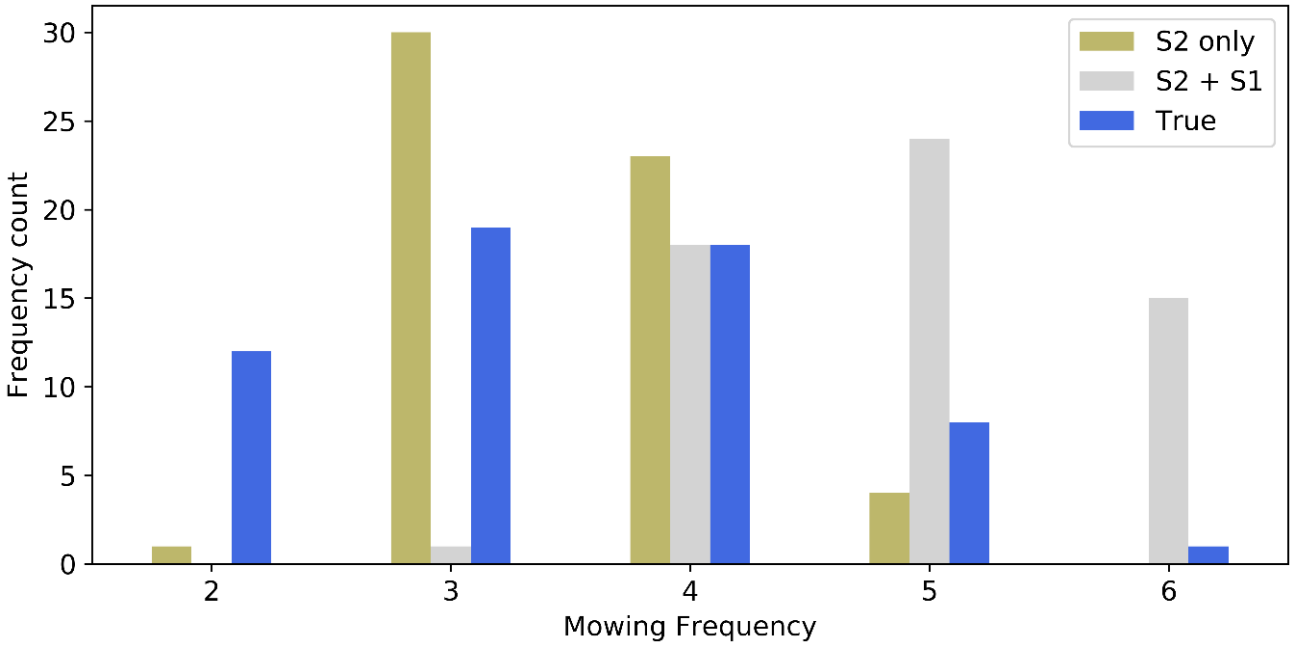

Figure 6. Detected mowing frequency of grassland reference parcels within the focus region when using S2 only and the combined approach consisting of S1 and S2, compared to the true condition.

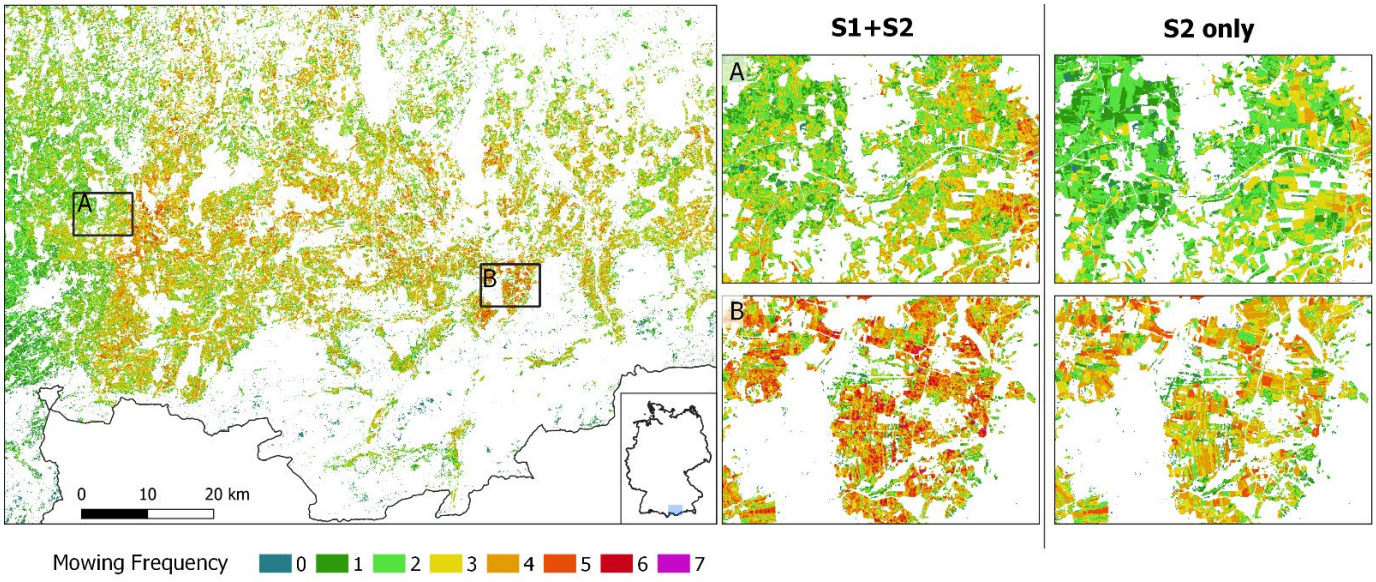

Figure 7. Mowing frequency derived from combined mowing detection approach of EVI and PolSAR entropy time series for the focus region and two zooms (A and B) with the frequency of the combined approach and only using S2.

For parcels with continuous validation information, in total 179 of 283 mowing events were correctly detected (63.3%) with an allowed time difference of seven days (Table 3). A total of 94 falsely detected events occurred (F1-Score = 0.64). Almost half of the false positives appeared on parcels that were also grazed.

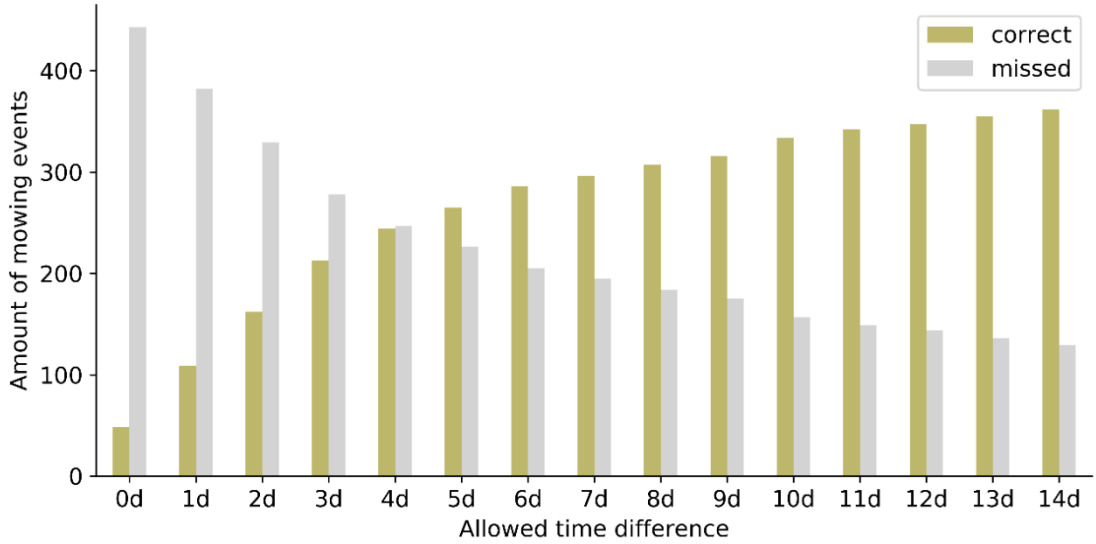

Figure 8. Number of correctly detected and missed mowing events depending on the allowed time difference between detection and actual mowing date.

Table 3. Accuracy matrix of detected mowing events in Germany showing successfully detected, missed events, and false positives.

		Actual Condition (Validation)	
		Mown	**Not Mown**
Predicted Condition (Satellite-based detection)	Mown	179	94
	Not mown	104	
Total		283	

The mowing frequency of the validation parcels with a complete data set (n (parcels) = 89, n (mowing events) = 283) was correct for 20% of the parcels. For 54% of these validation parcels, the difference between the detected and the actual mowing frequency was one. Overall, the mowing frequency was underestimated (Figure 9).

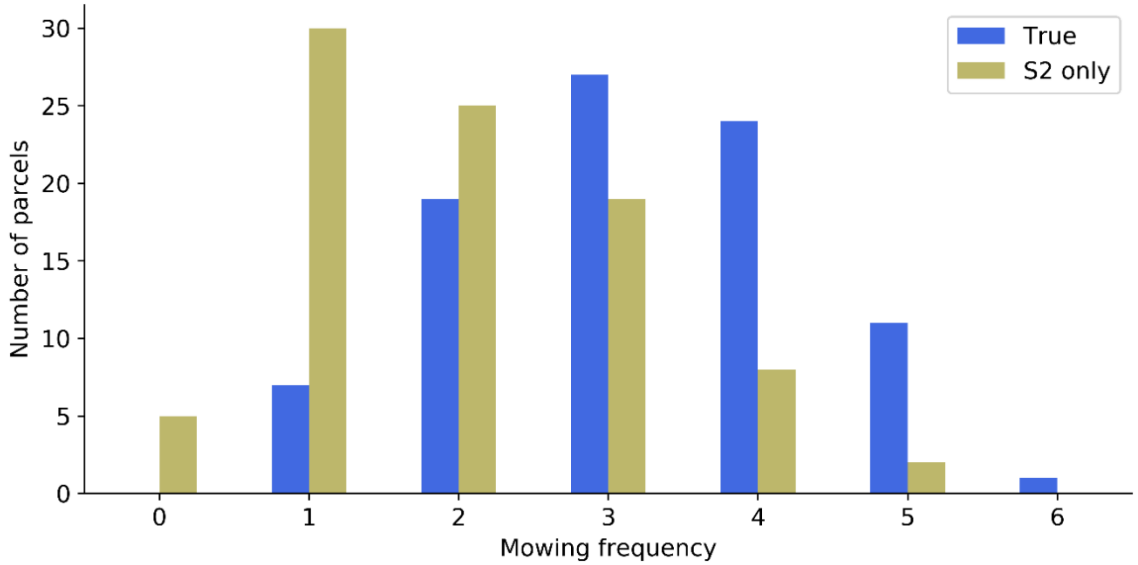

Figure 9. Number of mowing events per year from the validation dataset and detected for grassland parcels with continuous management information.

4.4. Germany-Wide Application of S2-Based Mowing Event Detection

The spatial patterns of the mowing frequency on the pixel level (Figure 10) show that many grasslands in the south-east and the very north of Germany are managed intensively with a high frequency of mowing events. In particular, within the valley of the river Inn in the south-eastern part of Germany (east of Figure 10c), the amount of grasslands that are mown often (more than four times) is high. Grasslands in the north-west display a median mowing frequency and parcels in the east and center of Germany are mown less often. Overall, the number of grasslands that are mown zero (13%), one (38%), or two times (33%) is relatively high in Germany (Figure 11). Intensively used grasslands that are mown four to six times account only for about 3%. While observing the mowing frequency for the whole of Germany (Figure 10), a systematic underestimation of the S2-based detection approach in regions with lower S2 orbit coverage is visible.

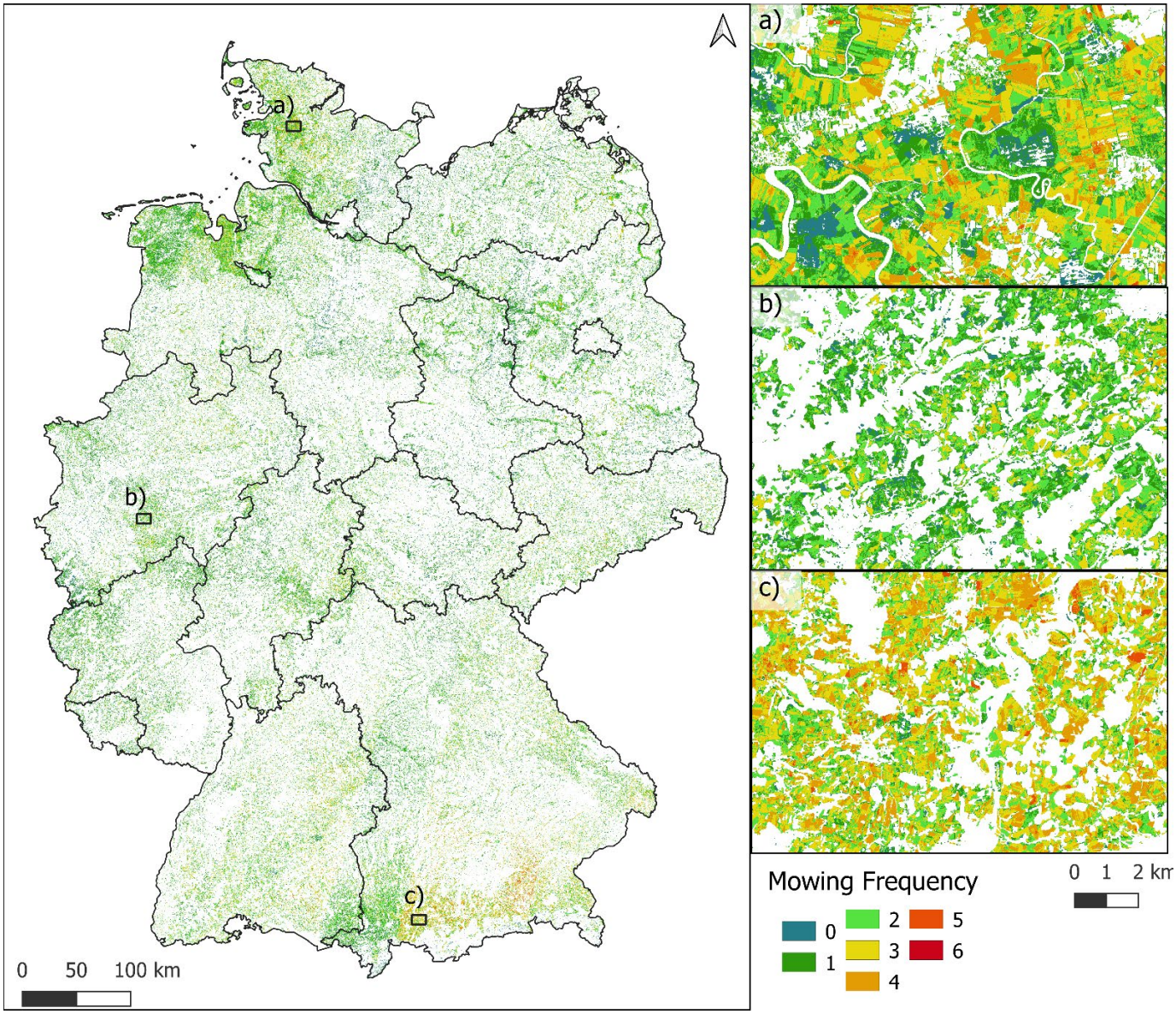

Figure 10. Mowing frequency 2019 on grassland with a spatial resolution of 10 m based on EVI time series data for Germany and for three zoom regions (a, b, c) indicated on the map.

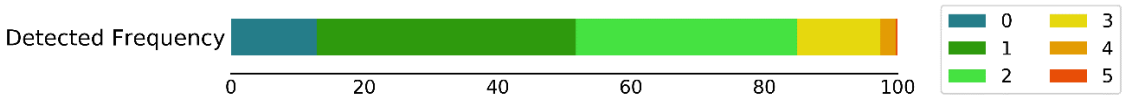

Figure 11. Number of grassland pixels with detected mowing frequency for Germany in percentage.

The timing of the first mowing event of 2019 (Figure 12) shows that grasslands in the south-east are mown early. Many grasslands are mown around the 1st of June, which is an ecologically critical date. For many plant species it is advantageous when the grassland parcel is mown around this date and therefore, this is also coupled to subsidiary payments in some federal states in Germany. These high-resolution maps show information on the pixel level and the parameters are not bound to parcel extents, which can vary during the year through partially differentiating use. However, single grassland sites are well distinguishable (Figures 10 and 12a–c).

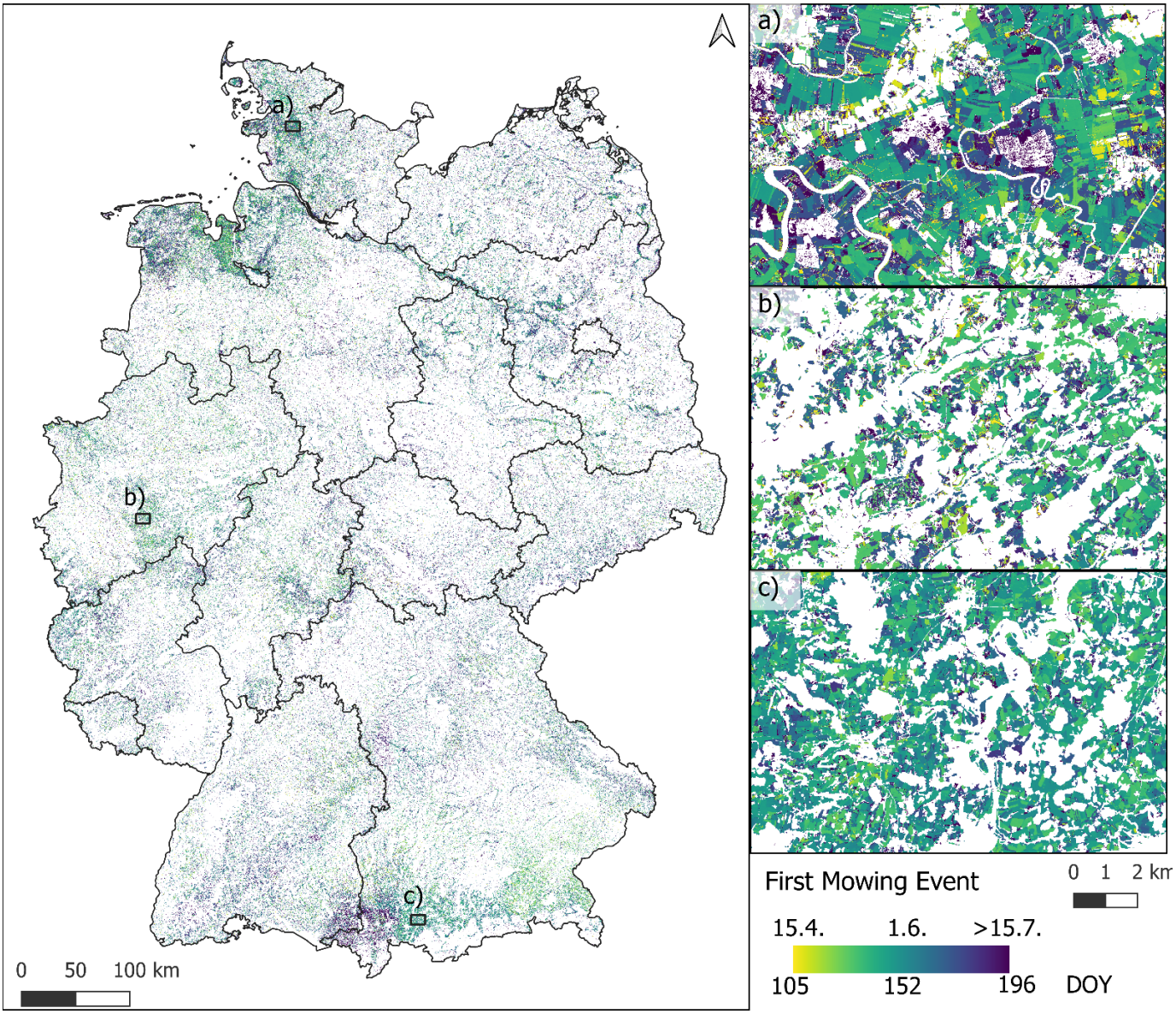

Figure 12. First mowing event on grassland in 2019 with a spatial resolution of 10 m with the EVI-based detection for Germany and for three zoom regions (a, b, c) indicated on the map.

On county level, the spatially aggregated information on intensively used grassland (mown four to six times), extensively used grasslands (mown zero to two times), and on the first mowing date reveal general patterns for Germany (Figure 13). The maps show the relative amount of grassland use intensities based on the entire grassland area per county ("Landkreis") in percentage. In particular, the grasslands in the south-east and the very north are intensively used (Figure 13A) and the grasslands in the center and north-east more extensively used (Figure 13B). The timing of the first mowing event reveals that—in addition to the areas of higher grassland mowing frequency in the south/south-east—the grasslands in western Germany are mown mainly before June 1st (Figure 13C). The number of available S2 scenes (i.e., due to overlapping swaths) seems to have the strongest influence on the extensively used grasslands (mown one to two times) (Figure 13B).

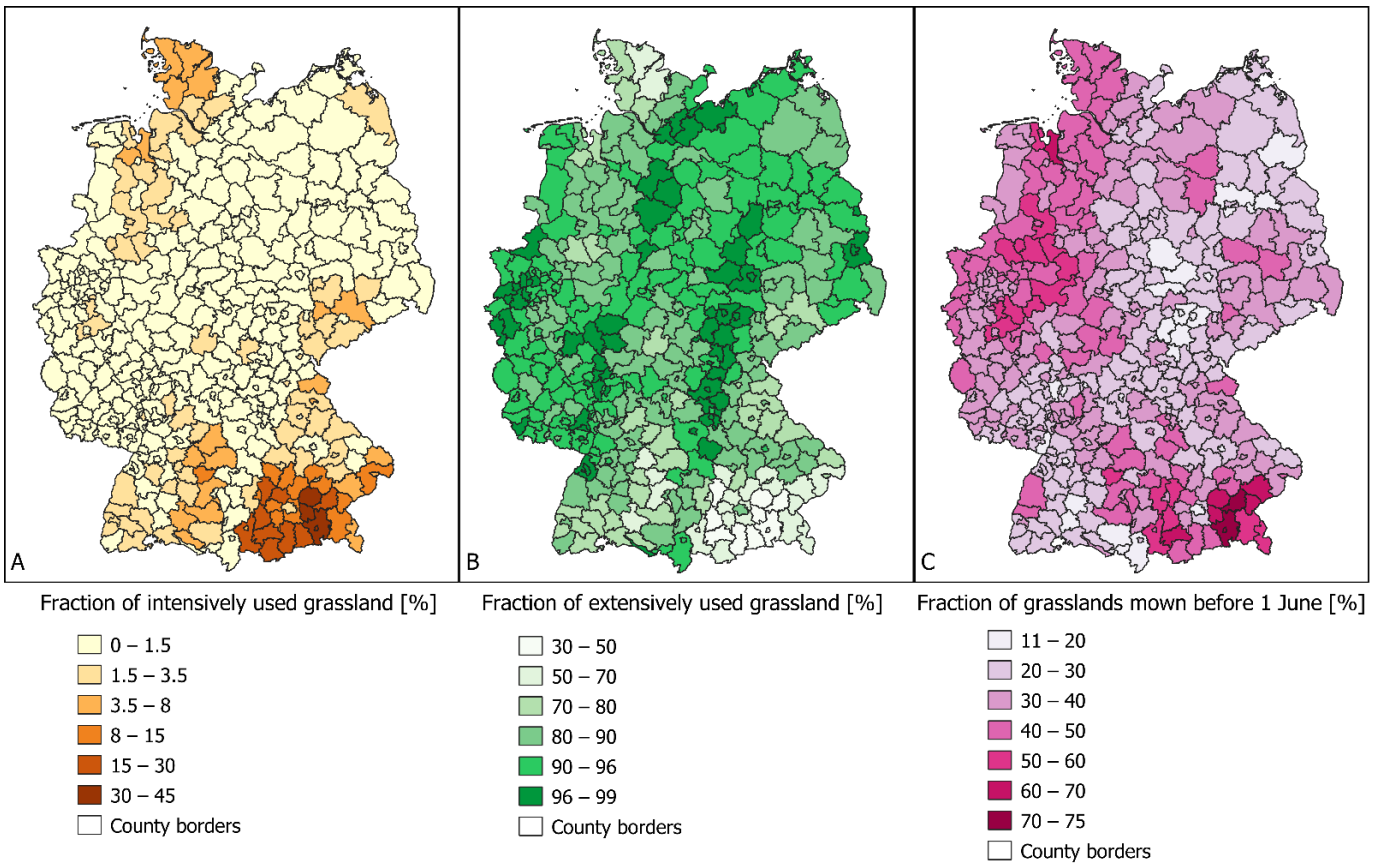

Figure 13. Fractions of grasslands within counties, which are used intensively (mown four to six times; (**A**)), extensively (mown zero to two times; (**B**)), and mown before the ecologically critical 1st of June (**C**).

The spatial patterns of the data availability and uncertainty information of the focus region partly overlap (Figure 14). The western part of the focus region, which is covered by only one S2 orbit swath, shows higher uncertainty (Figure 14B) and many cloud gaps (Figure 14A). The uncertainty shows higher values at field borders (Figure 14B).

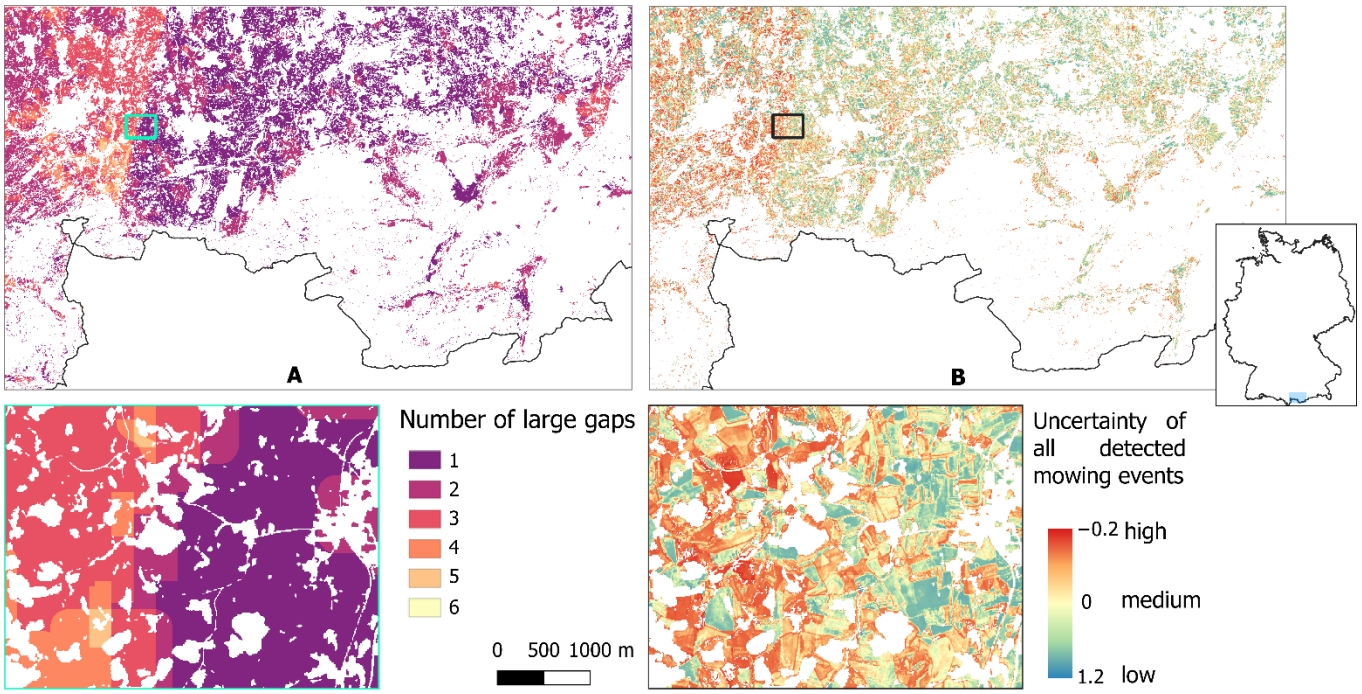

Figure 14. Quality information for the S2 dataset 2019 represented by the number of large gaps (**A**), and uncertainty information of the mowing frequency, estimated from the gradient and data availability of the detected mowing events (**B**) for the focus region (Ammer region) and a zoom region indicated on the map.

5. Discussion

5.1. Relationships between S1 and S2 Parameters and Mowing Events

5.1.1. The Relationship of S2-Based EVI to Mowing Events

In this study, the mowing events were detected through the analysis of S1 and S2 time series with the purpose to generate map products of the grassland mowing regime in Germany. The EVI time series shows a good relationship to the mowing event patterns. This is in accordance with other research, where significant drops (around 0.2 to 0.5) in raw NDVI time series data were found after mowing events in central Europe [18–20]. Here, we revealed that the exact threshold of the drop within the time series of the vegetation index, which is necessary to detect a mowing event, was not that important, as the successful detection of mowing events for the parametrization sites was almost equal for an EVI threshold range of 0.1 (from thresholds of 0.2 to 0.12 for th_1). The thresholding mechanism to detect mowing events is, therefore, sufficiently robust for a transfer to other grasslands, which show a temporal pattern of EVI drops, followed by increases after mowing activities. The major limiting factor of the S2-based grassland mowing detection is the data availability, which is limited by orbit and cloud coverage. Only when dense optical time series are available, mowing detections are successful, especially because the effects of the events are only visible for a short period of time (10 to 14 days). In particular in central Europe, grasslands occur mainly in moist [54] regions—in Germany, these are often mountainous or coastal areas (Figure 1). These regions potentially experience relatively high cloud coverage during the year, which makes remote sensing-based grassland monitoring more difficult than in regions with less cloud cover.

In order to minimize the risk of missing mowing events due to data gaps, one solution might be to include more satellite datasets into the detection approach. The inclusion of SAR-based data, which was investigated within this study, is discussed in the following paragraphs. However, it might be also useful to add optical data from different sources [17,20,33]. Additional optical data (e.g., Landsat, PlanetScope) has the potential to

fill up the time series and reduce the amount of critical data gaps. However, one obstacle of combining optical datasets from multiple sources is the need of harmonization. Especially when short-lived temporal patterns on the pixel scale are investigated, spectral differences within the time series arising from variations in radiometry, spatial resolution or acquisition geometry of the sensors are problematic. In addition, the spatial resolution might be reduced by adding data with lower resolution, as usually is the case for the combined dataset from S2 and Landsat 8, which has a spatial resolution of 30 m. Lastly, all optical satellite data have the same limitation in the appearance of clouds. If the mowing event happens during cloudy conditions and the brief local minimum within the optical time series is therefore not recorded, no additional optical dataset can lead to an improvement.

Another valuable observation from the examination of the parametrization parcels within this study are the temporal patterns of grazing events, as the occurrence of cows was tracked with the cameras, next to the mowing event. For extensive parcels, which are grazed and only mown once, single grazing events lead to a less abrupt and long-lasting decrease in EVI (Figure 5: HF). Nevertheless, these grazing events were at times confused with mowing events, as an EVI decrease was detected by the algorithm (e.g., Figure 5: HF). As this gradient of EVI decrease is part of the uncertainty layer, which was developed within this study (Section 3.4, Figure 14), this layer might be used to filter grazing events, which were falsely detected as mowing events in a post-processing approach. However, in the cases of the parametrization parcels, the number of cows was relatively low. It is assumed that parcels that are grazed with higher stocking rates show a faster EVI decrease, and the grazing event would be harder to differentiate from a mowing event.

5.1.2. The Relationship of S1-Based Backscatter to Mowing Events

To complement the mowing detection, SAR-based parameters were investigated within this study. The S1 VV and VH intensities show only small and not consistent reactions to the mowing regime. Some studies found an increase in the temporal backscatter signal after mowing events [21,22,55], which, however, could not be confirmed in this study (Section 3.2.1). Our results are thus in line with other studies that did not find a visual or statistical relationship between SAR backscatter and the mowing regime [27,31]. The reason that the backscatter signal only rarely shows a reaction after mowing events might be that the effect of scattering mechanisms is different than anticipated. Initially, it was assumed that the backscatter increases after mowing events as these provoke a shift from volume scattering of large and dense canopies to surface scattering from short vegetation and soil [56]. However, in many cases the mown grass remains on the parcel for several days for drying. This might result in volume scattering and a missing immediate increase in the backscatter.

5.1.3. The Relationship of S1-Based InSAR Coherence to Mowing Events

Regarding InSAR, the VV coherence and VH coherence revealed a relationship to the mowing regime within this study. However, the temporal signal seems to be additionally influenced by other drivers than the grassland management as peaks unrelated to mowing events are visible, which is in accordance with the findings of previous studies ([26,27] for COSMO-Skymed; [29] for TerraSAR-X; [31] for S1). In addition, the value ranges of the coherence parameters are close to the noise level [57], making an inclusion of these parameters into a mowing detection algorithm less reliable. A potential explanation for the relationship between the InSAR coherence signal and the grassland mowing regime is that vegetation growth, an increase in density, and motion of vegetation cause a decorrelation (e.g., [31]). Therefore, a continuous decrease in InSAR coherence is assumed during the growing phase. After a mowing event, the coherence potentially abruptly drops, when the image pair consists of one image from before the event and one from afterwards. Or—with both images from after the mowing event—the coherence increases due to more stable influence from the soil and less from the vegetation. Besides mowing events, precipitation is assumed to strongly influence the coherence signal as an increase in plant and soil

moisture is a reason for increased decorrelation. However, the growth phase probably additionally influences these effects [31], as the effect of drivers on the InSAR coherence signal probably varies with different phenological stages, e.g., [49]. In addition, the InSAR coherence is special as it already consists of a comparison of two images. As the effects of potential drivers can influence both or only one image, general assumptions are additionally complicated. It is needed to differentiate between the reactions of the signal when the precipitation event, for example, happened before, during, or after the 12-day comparison period of the acquisitions.

5.1.4. The Relationship of S1-Based PolSAR Decomposition Parameters to Mowing Events

PolSAR decomposition parameters were, until now, only investigated with TerraSAR-X and Radarsat-2 regarding their relationship to grassland mowing [25,28]. Similar to our results, these studies found an increase in PolSAR entropy after mowing events, which was inconsistent. The increase in PolSAR entropy might result from a shift in the orientation of the scatters. While growing grass is probably more vertically oriented, mown grass on the ground is horizontally oriented, which results in a higher depolarization.

5.2. Spatial Patterns of Detected Mowing Events in Germany

The mowing frequency map of Germany based on S2 carries high-resolution management information. Even though the approach is conducted on a pixel basis, the extents of single grassland parcels are visible, indicating the robustness of the approach. The advantage of a pixel-based detection algorithm is that the mowing event detection is not disturbed when the parcels are not completely mown within one day or when they are partly used for grazing for some days or weeks. The analysis of the mowing event detection, and in particular the investigation of the camera-based reference information, showed that some parts of parcels are sometimes not mown or are used differently.

The spatial patterns of the mowing frequency reveal that grassland parcels in the very south, the south-east, and the north of Germany are mown more often than in other parts of Germany in 2019. This general pattern is in accordance with detected mowing frequencies of Germany in a recent study [17]. The pattern might be related to more moisture availability and hence increased growth rate and biomass there. In fact, the regions with high proportions of grasslands mown four to six times per year in the south, south-east, and north and the more intensively used grasslands in North Rhine-Westphalia (north-west of Germany), characterized by a large proportion of grasslands mown before 1st of June, show similar climatic conditions [54]. These are characterized by average temperatures of more than 10 °C for at least five month per year and relatively high precipitation rates of 1000 to 1500 mm per year [58]. However, grassland management is not only determined by site conditions, such as climate, but can have multiple reasons. The accessibility, soil quality, and the individual decisions of farmers play a role as well. The investigation of the timing of the first mowing event shows that many grassland parcels are mown around the 1st of June. The timing of the first mowing event plays an important role for richness and distribution of grassland species and the species richness is higher when grasslands are mown rather later in spring/beginning of summer (around 1st of June). For many naturally occurring grassland plant species, mowing before June leads to a local extinction [4,6] as they are unable to reach the phenological stage enabling reproduction. The spatial pattern of the timing of the first mowing event relates to the mowing frequency as grasslands that are mown more often are also mown earlier (see [59]).

Apart from local management patterns, the national maps of mowing frequency and the timing of the first mowing events based on S2 indicate an influence of the availability of optical data. When comparing these maps to the amount of valid optical observations (Figure 2), fewer mowing events were detected in the regions that are only covered by one S2 orbit. The reason for that is that with only one orbit coverage, the probability of valid observations is half and hence the probability of missing harvests increases. This becomes

also visible within the quality layer created within this study that represents the amount of large data gaps due to cloud cover (Figure 14).

5.3. Importance and Drawbacks of Optical and SAR Data Fusion

Selected parameters based on S1 and S2 often show visible effects of mowing activities within their temporal profiles and combining indicators from both sources—optical and SAR—might be advantageous in order to guarantee a more complete mowing detection by reducing missed events due to clouds. Voormansik et al. [31] found no strong correlation between InSAR coherence and NDVI for grasslands. This either indicates that S1 and S2 time series are influenced by multiple and potentially different drivers other than the mowing regime, or that they should be rather used as complementary information for mowing detection.

Here, we applied and discussed an empirical threshold-based combination of S1 and S2 mainly to fill cloud-induced gaps and retrieve potentially missed mowing events. S1 information is only used when S2 data is not available as the effects of the mowing events visible within S1 parameters were not as consistent and straightforward as they are for S2. The approach of filling periods of unfavorable atmospheric conditions limiting optical observations with SAR data is used in various fields, for example for the detection of surface water [60]. However, within this study, the combined approach (S2 + S1) did not improve the grassland mowing detection as the increased number of successful detections was accompanied by a rise in false positives. Lobert et al. [33] combined S1 and S2 data in a deep learning classification approach (convolutional neural network) to detect mowing events. The model based on NDVI, backscatter cross-ratio, and InSAR coherence led to the best results (F1-Score = 0.84). The NDVI time series consisted of data from S2 and Landsat 8, and the approach was only tested for areas with overlapping S2 orbits (compare Figure 2). The time series of valid NDVI was, therefore, presumably relatively dense and it is yet to be tested if the SAR data are a valuable source for regions with less continuous optical data information within their approach.

Here, the PolSAR entropy was identified in a comprehensive comparison of seven SAR-based parameters as the best S1-based indicator to complement the mowing detection approach conducted with S2 EVI. Adding PolSAR entropy to a deep learning classification model for mowing detection might improve the results and has still to be investigated in future research. Adding additional potential drivers, such as precipitation, might improve the performance of SAR-based parameters to detect mowing events.

6. Conclusions

Our analyses show that with dense optical time series, diverse grassland mowing regimes in Germany can be successfully characterized by the derivation of mowing dates and mowing frequency. However, cloud gaps and lower S2 coverage are potentially problematic, in particular as the reaction of the vegetation index is usually only detectable for a short time period (10 to 14 days).

- The detection of grassland mowing events is possible with optical data; however, only if dense time (period < 10 to 14 days) series are available;
- A pixel-based approach is possible and advantageous as parcels are at times not used homogenously;
- The temporal signal of InSAR and PolSAR parameters for mown grasslands are inconsistent and do not reveal a clear relation to mowing events. Most probably they depend on additional drivers (i.e., moisture), for which general assumptions are difficult to make;
- Complementing the optical mowing detection approach based on EVI time series by the PolSAR entropy, led to an increase in detected mowing events by 9.2%. However, more false positives also occurred, resulting in a drop of the F1-Score (F1-Score = 0.65 for S2 only, F1-Score = 0.61 for S2 + S1);

- Use intensity and timing of the first mowing event of grasslands in Germany are heterogeneously distributed with more often mown parcels in the south/south-east and the north;
- In Germany, 13% of grasslands are not mown at all and a majority is only mown one (38%) to two times (33%), which might be grazed as well. Only 3% of all grasslands are mown four to six times, according to our analysis.

Supplementary Materials: The following supporting information can be downloaded at: https://www.mdpi.com/article/10.3390/rs14071647/s1, Table S1: Description of exemplary sites, Table S2: List of webcam websites, Figure S3: Example of public webcam, Table S4: Information on calibration sites, Figure S5: Pre-processing flowchart of S1 and S2 parameters, Figure S6: Comparison of values before and after mowing events for all investigated parameters.

Author Contributions: Conceptualization, S.A., S.R., U.G. and C.K.; methodology, S.R.; software, S.R. and T.U.; validation, S.R. and A.S.; formal analysis, S.R.; investigation, S.R.; writing—original draft preparation, S.R.; writing—review and editing, S.R., S.A., U.G., T.U., A.S. and C.K.; visualization, S.R.; supervision, C.K.; project administration, S.R. and S.A.; funding acquisition, S.A. All authors have read and agreed to the published version of the manuscript.

Funding: This research was conducted within the SUSALPS project (https://www.susalps.de/, accessed on 22 March 2022) funded by the German Federal Ministry for Education and Research (BMBF), grant number 031B0516F.

Data Availability Statement: Not applicable.

Acknowledgments: We thank the anonymous reviewers for their helpful comments. In addition, we would like to thank the Copernicus program of the European Environmental Agency for providing open access data on grassland land cover (Grassland HRL) and the EU-DEM.

Conflicts of Interest: The authors declare no conflict of interest.

References

1. Reynolds, S.; Frame, J. *Grasslands: Developments, Opportunities, Perspectives*; Food & Agriculture Organization: Rome, Italy, 2005.
2. White, R.P.; Murray, S.; Rohweder, M. *Pilot Analysis of Global Ecosystems—Grassland Ecosystems*; World Resources Institute: Washington, DC, USA, 2000.
3. Bengtsson, J.; Bullock, J.M.; Egoh, B.; Everson, C.; Everson, T.; O'Connor, T.; O'Farrell, P.J.; Smith, H.G.; Lindborg, R. Grasslands-more important for ecosystem services than you might think. *Ecosphere* **2019**, *10*, e02582. [CrossRef]
4. Schoof, N.; Luick, R.; Ackermann, A.; Baum, S.; Böhner, H.; Röder, N.; Rudolph, S.; Schmidt, T.G.; Hötker, H.; Jeromin, H. (Eds.) *Auswirkungen der Neuen Rahmenbedingungen der Gemeinsamen Agrarpolitik Auf Die Grünland-Bezogene Biodiversität*, 2nd ed.; BfN-Skripten; Bundesamt für Naturschutz: Bonn, Germany, 2020; Volume 540, ISBN 978-3-89624-278-5.
5. Poeplau, C.; Jacobs, A.; Don, A.; Vos, C.; Schneider, F.; Wittnebel, M.; Tiemeyer, B.; Heidkamp, A.; Prietz, R.; Flessa, H. Stocks of organic carbon in German agricultural soils—Key results of the first comprehensive inventory. *J. Plant Nutr. Soil Sci.* **2020**, *183*, 665–681. [CrossRef]
6. Dengler, J.; Janišová, M.; Török, P.; Wellstein, C. Biodiversity of Palaearctic grasslands: A synthesis. *Agric. Ecosyst. Environ.* **2014**, *182*, 1–14. [CrossRef]
7. Zhang, Y.; Loreau, M.; He, N.; Zhang, G.; Han, X. Mowing exacerbates the loss of ecosystem stability under nitrogen enrichment in a temperate grassland. *Funct. Ecol.* **2017**, *31*, 1637–1646. [CrossRef]
8. Smith, A.L.; Barrett, R.L.; Milner, R.N.C. Annual mowing maintains plant diversity in threatened temperate grasslands. *Appl. Veg. Sci.* **2018**, *21*, 207–218. [CrossRef]
9. Bernhardt-Römermann, M.; Römermann, C.; Sperlich, S.; Schmidt, W. Explaining grassland biomass–the contribution of climate, species and functional diversity depends on fertilization and mowing frequency. *J. Appl. Ecol.* **2011**, *48*, 1088–1097. [CrossRef]
10. Gilmullina, A.; Rumpel, C.; Blagodatskaya, E.; Chabbi, A. Management of grasslands by mowing versus grazing—impacts on soil organic matter quality and microbial functioning. *Appl. Soil Ecol.* **2020**, *156*, 103701. [CrossRef]
11. Senapati, N.; Chabbi, A.; Gastal, F.; Smith, P.; Mascher, N.; Loubet, B.; Cellier, P.; Naisse, C. Net carbon storage measured in a mowed and grazed temperate sown grassland shows potential for carbon sequestration under grazed system. *Carbon Manag.* **2014**, *5*, 131–144. [CrossRef]
12. Schoof, N.; Luick, R.; Beaufoy, G.; Jones, G.; Einarsson, P.; Ruiz, J.; Stefanova, V.; Fuchs, D.; Windmaißer, T.; Hötker, H.; et al. (Eds.) *Grünlandschutz in Deutschland: Treiber der Biodiversität, Einfluss von Agrarumwelt-und Klimamaßnahmen, Ordnungsrecht, Molkereiwirtschaft und Auswirkungen der Klima-und Energiepolitik*, 2nd ed.; BfN-Skripten; Bundesamt für Naturschutz: Bonn, Germany, 2020; Volume 539, ISBN 978-3-89624-277-8.

13. Socher, S.A.; Prati, D.; Boch, S.; Müller, J.; Klaus, V.H.; Hölzel, N.; Fischer, M. Direct and productivity-mediated indirect effects of fertilization, mowing and grazing on grassland species richness. *J. Ecol.* **2012**, *100*, 1391–1399. [CrossRef]
14. Hilpold, A.; Seeber, J.; Fontana, V.; Niedrist, G.; Rief, A.; Steinwandter, M.; Tasser, E.; Tappeiner, U. Decline of rare and specialist species across multiple taxonomic groups after grassland intensification and abandonment. *Biodivers. Conserv.* **2018**, *27*, 3729–3744. [CrossRef]
15. European Commission Regulation (EU) No 1305/2013 of the European Parliament and of the Council of 17 December 2013 on support for rural development by the European Agricultural Fund for Rural Development (EAFRD) and repealing Council Regulation (EC) No 1698/2005. *Off. J. Eur. Union L* **2013**, *347*, 487–548.
16. Reinermann, S.; Asam, S.; Kuenzer, C. Remote Sensing of Grassland Production and Management—A Review. *Remote Sens.* **2020**, *12*, 1949. [CrossRef]
17. Schwieder, M.; Wesemeyer, M.; Frantz, D.; Pfoch, K.; Erasmi, S.; Pickert, J.; Nendel, C.; Hostert, P. Mapping grassland mowing events across Germany based on combined Sentinel-2 and Landsat 8 time series. *Remote Sens. Environ.* **2021**, *9*, 112795. [CrossRef]
18. Courault, D.; Hadria, R.; Ruget, F.; Olioso, A.; Duchemin, B.; Hagolle, O.; Dedieu, G. Combined use of FORMOSAT-2 images with a crop model for biomass and water monitoring of permanent grassland in Mediterranean region. *Hydrol. Earth Syst. Sci. Discuss.* **2010**, *14*, 1731–1744. [CrossRef]
19. Kolecka, N.; Ginzler, C.; Pazur, R.; Price, B.; Verburg, P.H. Regional Scale Mapping of Grassland Mowing Frequency with Sentinel-2 Time Series. *Remote Sens.* **2018**, *10*, 1221. [CrossRef]
20. Griffiths, P.; Nendel, C.; Pickert, J.; Hostert, P. Towards national-scale characterization of grassland use intensity from integrated Sentinel-2 and Landsat time series. *Remote Sens. Environ.* **2020**, *238*, 111124. [CrossRef]
21. Schuster, C.; Ali, I.; Lohmann, P.; Frick, A.; Foerster, M.; Kleinschmit, B. Towards Detecting Swath Events in TerraSAR-X Time Series to Establish NATURA 2000 Grassland Habitat Swath Management as Monitoring Parameter. *Remote Sens.* **2011**, *3*, 1308–1322. [CrossRef]
22. Grant, K.; Siegmund, R.; Wagner, M.; Hartmann, S. Satellite-based assessment of grassland yields. *Int. Arch. Photogramm. Remote Sens. Spat. Inf. Sci.* **2015**, *40*, 15. [CrossRef]
23. Taravat, A.; Wagner, M.P.; Oppelt, N. Automatic Grassland Cutting Status Detection in the Context of Spatiotemporal Sentinel-1 Imagery Analysis and Artificial Neural Networks. *Remote Sens.* **2019**, *11*, 711. [CrossRef]
24. De Vroey, M.; Radoux, J.; Defourny, P. Grassland Mowing Detection Using Sentinel-1 Time Series: Potential and Limitations. *Remote Sens.* **2021**, *13*, 348. [CrossRef]
25. Voormansik, K.; Jagdhuber, T.; Olesk, A.; Hajnsek, I.; Papathanassiou, K.P. Towards a detection of grassland cutting practices with dual polarimetric TerraSAR-X data. *Int. J. Remote Sens.* **2013**, *34*, 8081–8103. [CrossRef]
26. Zalite, K.; Voormansik, K.; Praks, J.; Antropov, O.; Noorma, M. *Towards Detecting Mowing of Agricultural Grasslands from Multi-Temporal COSMO-SkyMed Data*; IEEE Geoscience and Remote Sensing Symposium: Quebec City, QC, Canada, 2014; pp. 5076–5079.
27. Zalite, K.; Antropov, O.; Praks, J.; Voormansik, K.; Noorma, M. Monitoring of agricultural grasslands with time series of X-band repeat-pass interferometric SAR. *IEEE J. Sel. Top. Appl. Earth Obs. Remote Sens.* **2015**, *9*, 3687–3697. [CrossRef]
28. Voormansik, K.; Jagdhuber, T.; Zalite, K.; Noorma, M.; Hajnsek, I. Observations of cutting practices in agricultural grasslands using polarimetric SAR. *IEEE J. Sel. Top. Appl. Earth Obs. Remote Sens.* **2015**, *9*, 1382–1396. [CrossRef]
29. Ali, I.; Barrett, B.; Cawkwell, F.; Green, S.; Dwyer, E.; Neumann, M. Application of Repeat-Pass TerraSAR-X staring spotlight interferometric coherence to monitor pasture biophysical parameters: Limitations and sensitivity analysis. *IEEE J. Sel. Top. Appl. Earth Obs. Remote Sens.* **2017**, *10*, 3225–3231. [CrossRef]
30. Tamm, T.; Zalite, K.; Voormansik, K.; Talgre, L. Relating Sentinel-1 interferometric coherence to mowing events on grasslands. *Remote Sens.* **2016**, *8*, 802. [CrossRef]
31. Voormansik, K.; Zalite, K.; Sünter, I.; Tamm, T.; Koppel, K.; Verro, T.; Brauns, A.; Jakovels, D.; Praks, J. Separability of Mowing and Ploughing Events on Short Temporal Baseline Sentinel-1 Coherence Time Series. *Remote Sens.* **2020**, *12*, 3784. [CrossRef]
32. Stendardi, L.; Karlsen, S.R.; Niedrist, G.; Gerdol, R.; Zebisch, M.; Rossi, M.; Notarnicola, C. Exploiting Time Series of Sentinel-1 and Sentinel-2 Imagery to Detect Meadow Phenology in Mountain Regions. *Remote Sens.* **2019**, *11*, 542. [CrossRef]
33. Lobert, F.; Holtgrave, A.-K.; Schwieder, M.; Pause, M.; Vogt, J.; Gocht, A.; Erasmi, S. Mowing event detection in permanent grasslands: Systematic evaluation of input features from Sentinel-1, Sentinel-2, and Landsat 8 time series. *Remote Sens. Environ.* **2021**, *267*, 112751. [CrossRef]
34. Tischew, S.; Hölzel, N. Wirtschaftsgrünland. In *Renaturierungsökologie*; Kollmann, J., Kirmer, A., Tischew, S., Hölzel, N., Kiehl, K., Eds.; Springer: Berlin/Heidelberg, Germany, 2019; Volume 94, pp. 349–368, ISBN 978-3-662-54912-4.
35. Klaus, V.H.; Boch, S.; Boeddinghaus, R.S.; Hölzel, N.; Kandeler, E.; Marhan, S.; Oelmann, Y.; Prati, D.; Regan, K.M.; Schmitt, B.; et al. Temporal and small-scale spatial variation in grassland productivity, biomass quality, and nutrient limitation. *Plant Ecol.* **2016**, *217*, 843–856. [CrossRef]
36. Copernicus High Resolution Layer—Grassland 2018. Available online: https://land.copernicus.eu/pan-european/high-resolution-layers/grassland/status-maps/grassland-2018 (accessed on 1 April 2019).
37. Koeppen, W. Das geographische System der Klimate. In *Handbuch der Klimatologie*; Koeppen, W., Geiger, R., Eds.; Gebrueder Borntraeger: Berlin, Germany, 1936; pp. 1–44.

38. Kiese, R.; Fersch, B.; Baessler, C.; Brosy, C.; Butterbach-Bahl, K.; Chwala, C.; Dannenmann, M.; Fu, J.; Gasche, R.; Grote, R.; et al. The TERENO Pre-Alpine Observatory: Integrating Meteorological, Hydrological, and Biogeochemical Measurements and Modeling. *Vadose Zone J.* **2018**, *17*, 180060. [CrossRef]
39. Sokolova, M.; Lapalme, G. A systematic analysis of performance measures for classification tasks. *Inf. Processing Manag.* **2009**, *45*, 427–437. [CrossRef]
40. Drusch, M.; Del Bello, U.; Carlier, S.; Colin, O.; Fernandez, V.; Gascon, F.; Hoersch, B.; Isola, C.; Laberinti, P.; Martimort, P.; et al. Sentinel-2: ESA's Optical High-Resolution Mission for GMES Operational Services. *Remote Sens. Environ.* **2012**, *120*, 25–36. [CrossRef]
41. Torres, R.; Snoeij, P.; Geudtner, D.; Bibby, D.; Davidson, M.; Attema, E.; Potin, P.; Rommen, B.; Floury, N.; Brown, M.; et al. GMES Sentinel-1 mission. *Remote Sens. Environ.* **2012**, *120*, 9–24. [CrossRef]
42. Hagolle, O.; Huc, M.; Desjardins, C.; Auer, S.; Richter, R. Maja Algorithm Theoretical Basis Document; V1.0. 2017. Available online: https://zenodo.org/record/1209633#.YkFuyvlByUk (accessed on 1 March 2022).
43. Huete, A.; Didan, K.; Miura, T.; Rodriguez, E.; Gao, X.; Ferreira, L. Overview of the radiometric and biophysical performance of the MODIS vegetation indices. *Remote Sens. Environ.* **2002**, *83*, 195–213. [CrossRef]
44. Savitzky, A.; Golay, M.J.E. Smoothing and Differentiation of Data by Simplified Least Squares Procedures. *Anal. Chem.* **1964**, *36*, 1627–1639. [CrossRef]
45. Copernicus EU-DEM: v1.1 2016. Available online: https://land.copernicus.eu/imagery-in-situ/eu-dem/eu-dem-v1.1 (accessed on 8 February 2022).
46. Schmitt, A.; Wendleder, A.; Hinz, S. The Kennaugh element framework for multi-scale, multi-polarized, multi-temporal and multi-frequency SAR image preparation. *ISPRS J. Photogramm. Remote Sens.* **2015**, *102*, 122–139. [CrossRef]
47. Ullmann, T.; Banks, S.N.; Schmitt, A.; Jagdhuber, T. Scattering Characteristics of X-, C- and L-Band PolSAR Data Examined for the Tundra Environment of the Tuktoyaktuk Peninsula, Canada. *Appl. Sci.* **2017**, *7*, 595. [CrossRef]
48. Cloude, S. The dual polarization entropy/alpha decomposition: A PALSAR case study. *Sci. Appl. SAR Polarim. Polarim. Interferom.* **2007**, *644*, 2.
49. Löw, J.; Ullmann, T.; Conrad, C. The Impact of Phenological Developments on Interferometric and Polarimetric Crop Signatures Derived from Sentinel-1: Examples from the DEMMIN Study Site (Germany). *Remote Sens.* **2021**, *13*, 2951. [CrossRef]
50. Ullmann, T.; Serfas, K.; Büdel, C.; Padashi, M.; Baumhauer, R. Data Processing, Feature Extraction, and Time-Series Analysis of Sentinel-1 Synthetic Aperture Radar (SAR) Imagery: Examples from Damghan and Bajestan Playa (Iran). *Z. Geomorphol. Suppl. Issues* **2019**, *62*, 9–39. [CrossRef]
51. Scheuchl, B.; Ullmann, T.; Koudogbo, F. Change detection using high resolution TerraSAR-X data: Preliminary results. *Int. Arch. Photogramm. Remote Sens. Spat. Inf. Sci.* **2009**, *38*, 1–47.
52. Zebker, H.A.; Villasenor, J. Others Decorrelation in interferometric radar echoes. *IEEE Trans. Geosci. Remote Sens.* **1992**, *30*, 950–959. [CrossRef]
53. Touzi, R.; Lopes, A.; Bruniquel, J.; Vachon, P.W. Coherence estimation for SAR imagery. *IEEE Trans. Geosci. Remote Sens.* **1999**, *37*, 135–149. [CrossRef]
54. Deutschland—Klimaregionen 2021. In *Diercke Weltatlas*; Westermann Bildungsmedien Verlag GmbH: Braunschweig, Germany, 2020; p. 54. ISBN 978-3-14-100800-5.
55. Grant, K.; Wagner, M.; Siegmund, R.; Hartmann, S. The use of radar images for detecting when grass is harvested and thereby improve grassland yield estimates: Grassland Science in Europe, Grassland and Forages in High Output Dairy Farming Systems. In Proceedings of the Grassland Science in Europe, Grassland Science Federation, Wageningen, The Netherlands, 14–17 June 2015; Volume 20, pp. 419–421.
56. McNairn, H.; Brisco, B. The application of C-band polarimetric SAR for agriculture: A review. *Can. J. Remote Sens.* **2004**, *30*, 525–542. [CrossRef]
57. Wegmuller, U.; Werner, C. Retrieval of vegetation parameters with SAR interferometry. *IEEE Trans. Geosci. Remote Sens.* **1997**, *35*, 18–24. [CrossRef]
58. Annual Precipitation Germany 2020, German Weather Service (DWD). Available online: https://www.dwd.de/DE/leistungen/klimakartendeutschland/klimakartendeutschland.html?nn=16102 (accessed on 4 December 2021).
59. Gomez-Gimenez, M.; de Jong, R.; Peruta, R.D.; Keller, A.; Schaepman, M.E. Determination of grassland use intensity based on multi-temporal remote sensing data and ecological indicators. *Remote Sens. Environ.* **2017**, *198*, 126–139. [CrossRef]
60. Manakos, I.; Kordelas, G.A.; Marini, K. Fusion of Sentinel-1 data with Sentinel-2 products to overcome non-favourable atmospheric conditions for the delineation of inundation maps. *Eur. J. Remote Sens.* **2020**, *53*, 53–66. [CrossRef]